ORCA – Online Research @ Cardiff

This is an Open Access document downloaded from ORCA, Cardiff University's institutional repository:https://orca.cardiff.ac.uk/id/eprint/157666/

This is the author's version of a work that was submitted to / accepted for publication.

Citation for final published version:

Manoharan, Shathviga, Taylor-Joyce, Grace, Brooker, Thomas A., Hernández Rodríguez, Carmen Sara, Hapeshi, Alexia, Baldwin, Victoria, Baillie, Les ORCID: https://orcid.org/0000-0002-8186-223X, Oyston, Petra C. F. and Waterfield, Nicholas R. 2023. From cereus to anthrax and back again: Assessment of the temperature-dependent phenotypic switching in the "cross-over" strain Bacillus cereus G9241. Frontiers in Microbiology 14 10.3389/fmicb.2023.1113562 file

Publishers page: http://dx.doi.org/10.3389/fmicb.2023.1113562

Please note:
Changes made as a result of publishing processes such as copy-editing, formatting and page numbers may not be reflected in this version. For the definitive version of this publication, please refer to the published source. You are advised to consult the publisher's version if you wish to cite this paper.

This version is being made available in accordance with publisher policies. See http://orca.cf.ac.uk/policies.html for usage policies. Copyright and moral rights for publications made available in ORCA are retained by the copyright holders.

frontiers | Frontiers in Microbiology

TYPE Original Research
PUBLISHED 02 March 2023
DOI 10.3389/fmicb.2023.1113562

Check for updates

OPEN ACCESS

EDITED BY
Axel Cloeckaert,
Institut National de recherche pour l'agriculture (INRAE),
France

REVIEWED BY
Atmika Paudel,
Hokkaido University,
Japan
Didier Lereclus,
INRAE Centre Jouy-en-Josas,
France
Vitalii Timofeev,
State Research Center for Applied Microbiology and Biotechnology,
Russia

*CORRESPONDENCE
Nicholas R. Waterfield
✉ n.r.waterfield@warwick.ac.uk

SPECIALTY SECTION
This article was submitted to Infectious Agents and Disease, a section of the journal Frontiers in Microbiology

RECEIVED 01 December 2022
ACCEPTED 07 February 2023
PUBLISHED 02 March 2023

CITATION
Manoharan S, Taylor-Joyce G, Brooker TA, Hernández Rodríguez CS, Hapeshi A, Baldwin V, Baillie L, Oyston PCF and Waterfield NR (2023) From cereus to anthrax and back again: Assessment of the temperature-dependent phenotypic switching in the "cross-over" strain *Bacillus cereus* G9241. *Front. Microbiol.* 14:1113562.
doi: 10.3389/fmicb.2023.1113562

COPYRIGHT
© 2023 Manoharan, Taylor-Joyce, Brooker, Hernández Rodríguez, Hapeshi, Baldwin, Baillie, Oyston and Waterfield. This is an open-access article distributed under the terms of the Creative Commons Attribution License (CC BY). The use, distribution or reproduction in other forums is permitted, provided the original author(s) and the copyright owner(s) are credited and that the original publication in this journal is cited, in accordance with accepted academic practice. No use, distribution or reproduction is permitted which does not comply with these terms.

From cereus to anthrax and back again: Assessment of the temperature-dependent phenotypic switching in the "cross-over" strain *Bacillus cereus* G9241

Shathviga Manoharan[1], Grace Taylor-Joyce[1], Thomas A. Brooker[1], Carmen Sara Hernández Rodríguez[2], Alexia Hapeshi[1], Victoria Baldwin[3], Les Baillie[4], Petra C. F. Oyston[3] and Nicholas R. Waterfield[1]*

[1]Division of Biomedical Sciences, Warwick Medical School, University of Warwick, Coventry, United Kingdom, [2]Dpto. Microbiología y Ecología, Instituto BIOTECMED, Universitat de València, Burjassot, Spain, [3]CBR Division, Dstl Porton Down, Salisbury, United Kingdom, [4]School of Pharmacy and Pharmaceutical Sciences, Cardiff University, Cardiff, United Kingdom

Bacillus cereus G9241 was isolated from a Louisiana welder suffering from an anthrax-like infection. The organism carries two transcriptional regulators that have previously been proposed to be incompatible with each other in *Bacillus anthracis*: the pleiotropic transcriptional regulator PlcR found in most members of the *Bacillus cereus* group but truncated in all *B. anthracis* isolates, and the anthrax toxin regulator AtxA found in all *B. anthracis* strains and a few *B. cereus sensu stricto* strains. Here we report cytotoxic and hemolytic activity of cell free *B. cereus* G9241 culture supernatants cultured at 25°C to various eukaryotic cells. However, this is not observed at the mammalian infection relevant temperature 37°C, behaving much like the supernatants generated by *B. anthracis*. Using a combination of genetic and proteomic approaches to understand this unique phenotype, we identified several PlcR-regulated toxins to be secreted highly at 25°C compared to 37°C. Furthermore, results suggest that differential expression of the protease involved in processing the PlcR quorum sensing activator molecule PapR appears to be the limiting step for the production of PlcR-regulated toxins at 37°C, giving rise to the temperature-dependent hemolytic and cytotoxic activity of the culture supernatants. This study provides an insight on how *B. cereus* G9241 is able to "switch" between *B. cereus* and *B. anthracis*–like phenotypes in a temperature-dependent manner, potentially accommodating the activities of both PlcR and AtxA.

KEYWORDS

***Bacillus cereus* G9241, PlcR regulon, virulence factors, secretome, hemolysin**

Introduction

The *Bacillus cereus sensu lato* complex is a group of genetically similar but phenotypically diverse Gram-positive, soil-borne, rod-shaped bacteria (Vilain et al., 2006; Okinaka and Keim, 2016), which includes the well-studied *Bacillus anthracis and Bacillus cereus*. *B. anthracis* is the

etiological agent of anthrax (Carter, 1985) while *B. cereus* can colonize hosts as diverse as insects (Swiecicka and Mahillon, 2006) and humans, in which many strains can cause serious foodborne illness (Granum and Lund, 1997). Most members of the *B. cereus* group express the chromosomally encoded transcriptional regulator PlcR (Phospholipase C regulator), which controls the expression of many secreted degradative enzymes and toxins (Lereclus et al., 1996). However, the *plcR* gene in all *B. anthracis* isolates contains a point mutation, which frameshifts the gene and thus renders it non-functional (Agaisse et al., 1999). Previous studies have shown that inserting a functional copy of *plcR* in *B. anthracis* activates the PlcR regulon (Mignot et al., 2001; Pomerantsev et al., 2003, 2004). Mignot et al. (2001) demonstrated that *B. anthracis* Sterne (which has naturally lost its pXO2 plasmid) carrying a functional copy of the *Bacillus thuringiensis plcR* coding sequence and its promoter region in a plasmid led to expression of the PlcR regulon. However, this strain failed to sporulate within 24 h of inoculation while the wildtype and a *B. anthracis* strain lacking the pXO1 plasmid could sporulate at the same time point. This has led to the proposal that the acquisition of AtxA, the mammalian responsive transcriptional regulator involved in expressing anthrax toxins, is incompatible with the activity of PlcR, leading to a selection for PlcR mutation and inactivation (Agaisse et al., 1999; Mignot et al., 2001). Interestingly, a *B. cereus-B. anthracis* "cross-over" strain designated *B. cereus* G9241 (hereon referred to as *Bc*G9241) encodes intact copies of both *atxA* and *plcR* genes (Hoffmaster et al., 2004), suggesting this incompatibility dogma is not as straightforward as first suggested. One possibility that may explain compatibility of these regulators in *Bc*G9241 is the acquisition of compensatory mutation (s) allowing the coexistence of PlcR and AtxA.

*Bc*G9241 was isolated from a Louisiana welder, who was hospitalized with a respiratory infection resulting in a case of potentially lethal pneumonia (Hoffmaster et al., 2004). Symptoms were similar to those of inhalational anthrax. The patient also suffered with hemoptysis. *Bc*G9241 possesses three extrachromosomal elements: pBCX01, pBC210 and pBFH_1 (Hoffmaster et al., 2004, 2006). The plasmid pBCX01 shares 99.6% sequence homology with the plasmid pXO1 from *B. anthracis* strains. pBCX01 encodes the protective antigen (PA), lethal factor (LF), edema factor (EF) and the AtxA1 regulator. The second plasmid pBC210 (previously known as pBC218) encodes for the *B. cereus* exo-polysaccharide (BPS) capsule biosynthesis genes, *bpsXABCDEFGH* (Hoffmaster et al., 2004). A novel toxin named certhrax is also encoded on the pBC210 plasmid (Fieldhouse et al., 2010; Visschedyk et al., 2012), which has 31% amino acid sequence similarity with the LF from *B. anthracis*. Moreover, pBC210 encodes gene products with amino acid sequences bearing homology to AtxA and PA of *B. anthracis* (Hoffmaster et al., 2004). Subsequently these genes have been named *atxA2* and *pagA2*. The third extrachromosomal element pBFH_1 (previously known as pBClin29) is a linear phagemid (Hoffmaster et al., 2004). Although the sequence is available for pBFH_1, it is not known if it contributes to the lifestyle of *Bc*G9241. Our group demonstrated by transmission electron microscopy that the pBFH_1 phage could be produced and released into the supernatant (Taylor-Joyce et al., 2023). The shape of the phage particles and the dimensions of the tail and head appeared to be consistent with the Siphoviridae family (Hendrix et al., 2012), suggesting the pBFH_1 is a Siphoviridae phage. Phenotypically, *Bc*G9241 is hemolytic and resistant to γ-phage like other *B. cereus* strains (Hoffmaster et al., 2004). Further phenotypic and genetic analyses suggested that *Bc*G9241 should be considered a member of the *B. cereus sensu stricto* group as it does not encode a point mutation in the *plcR* gene indicative of all *B. anthracis* isolates (Mignot et al., 2001).

PlcR controls the expression of many secreted enzymes and toxins (Lereclus et al., 1996; Agaisse et al., 1999; Gohar et al., 2002), with at least 45 regulated genes found in *B. cereus* type strain ATCC 14579 (Gohar et al., 2008), hereon referred to as *Bc*ATCC14579. These secreted proteins, which contribute significantly to virulence in mice and insects (Salamitou et al., 2000), include hemolysins, enterotoxins, proteases, collagenases and phospholipases (Gohar et al., 2002). Activation of PlcR requires the binding of a secreted, processed and reimported form of the signaling peptide PapR (Lereclus et al., 1996; Økstad et al., 1999; Slamti et al., 2004; Bouillaut et al., 2008). The *papR* gene is located downstream of *plcR* and encodes a 48-amino acid protein. $PapR_{48}$ is secreted from the cell *via* the Sec machinery and processed to a heptapeptide by the extracellular zinc metalloprotease, NprB and potentially other extracellular proteases (Pomerantsev et al., 2009). The *nprB* gene is often tightly linked to the *plcR-papR* operon, but in the opposite orientation (Lereclus et al., 1996; Økstad et al., 1999; Pomerantsev et al., 2009). The processed form $PapR_7$ is reimported into the bacterium by the oligopeptide permease (Opp) system (Gominet et al., 2001). The processed form of PapR can then bind and activate PlcR. The active PlcR-PapR complex binds to the palindromic operator sequence (PlcR box: $TATGNAN_4TNCATA$) found in the promoter regions of the regulon genes, subsequently activating transcription of these genes (Slamti and Lereclus, 2002; Declerck et al., 2007; Grenha et al., 2013). PlcR also positively auto-regulates its own transcription, which can be repressed by the phosphorylated form of the sporulation factor Spo0A (Spo0A ~ P), facilitated by two Spo0A boxes flanking the PlcR box (Lereclus et al., 2000). Four distinct classes of PlcR-PapR systems have evolved and differ by the five C-terminal amino acids of PapR, which bind to PlcR, with PapR from one group unable to activate the transcriptional activity of PlcR from another (Slamti and Lereclus, 2005).

The chromosome of *Bc*G9241 encodes a large range of intact exotoxin genes confirming the strain is part of the *sensu stricto* group (Hoffmaster et al., 2004). Several of the toxin genes are likely to be regulated by PlcR, by virtue of the presence of the PlcR-box sequence in the promoter regions (Lereclus et al., 1996). These include hemolysin BL (Hbl) encoded by *hblCDAB*, the tripartite non-hemolytic enterotoxin (Nhe), encoded by *nheABC*, and the enterotoxin cytotoxin K (CytK), encoded by *cytK*. These three toxins are all classed as enterotoxins and are likely to be involved in the symptoms seen in food-borne, diarrhoeal infections (Gilmore et al., 1989; Lund and Granum, 1996; Lund et al., 2000). Since isolating *Bc*G9241, cases of anthrax-like disease caused by other non-*B. anthracis* strains have been reported, affecting both animals such as chimpanzees and gorillas in the Ivory Coast and Cameroon during the early 2000s (Leendertz et al., 2004, 2006a,b; Klee et al., 2010; Antonation et al., 2016), in addition to humans (Miller et al., 1997; Hoffmaster et al., 2004, 2006; Sue et al., 2006; Avashia et al., 2007; Wright et al., 2011; Marston et al., 2016; Pena-Gonzalez et al., 2017; Dupke et al., 2019; Dawson et al., 2021). Some of these isolates carry functional copies of *plcR* and *atxA* [recently reviewed in (Baldwin, 2020)]; this warrants further investigation into the role of PlcR in these strains, as the loss of PlcR activity has been proposed to be crucial in anthrax disease caused by *B. anthracis* (Mignot et al., 2001). So far, only one study on *Bc*G9241 has been carried out to identify how PlcR, AtxA, and their respective regulons are expressed. A microarray assay carried out by Passalacqua et al. (2009) demonstrated that in *Bc*G9241 the *plcR*

gene was ~2.4 fold more highly expressed in an aerobic environment compared to when exposed to CO_2/bicarbonate, while in contrast, the *atxA1* gene showed higher expression in CO_2 by ~5.6 fold. Understanding how the PlcR-PapR regulatory circuit acts in *B. cereus-B. anthracis* "cross-over" strains may provide an insight into their evolution and give a more complete picture of the phylogeny.

Here, we describe the temperature-dependent hemolytic and cytolytic activity of *Bc*G9241, caused by PlcR-controlled toxins and proteases. We also identify the limiting step in the PlcR-PapR circuit involved in preventing the expression of PlcR-regulated toxins at 37°C. NprB is not involved in processing PapR in *Bc*G9241 and other *B. cereus* strains carrying functional copies of both *plcR* and *atxA*. We hypothesize that a change in the PlcR-PapR regulatory network in *Bc*G9241 may have allowed the carriage of intact copies of both *plcR* and *atxA*, by virtue of a temperature-dependent suppression of the PlcR-PapR circuit and the loss of the *nprB* gene.

Results

*Bc*G9241 culture supernatants demonstrate temperature-dependent toxicity against a range of eukaryotic cells

It has been previously shown in other members of the *B. cereus* group that PlcR regulates the expression of genes encoding multiple exported virulence proteins, such as cytolytic toxins and enzymes involved in macromolecule degradation (Rivera et al., 2000; Swiecicka et al., 2006; Gohar et al., 2008). We therefore tested the hemolytic activity of cell free culture supernatants from *Bc*G9241 cultures grown at 25°C and 37°C to sheep erythrocytes. We tested the effect of growth at 25°C and 37°C to partially emulate environmental and mammalian host conditions, respectively. Filtered supernatants were extracted from cultures grown to mid-exponential phase ($OD_{600}=0.5$) and late stationary phase. For late stationary phase, *Bc*G9241 cultures supernatant were extracted after 10 h growth at 25°C and after 7 h growth at 37°C (Taylor-Joyce et al., 2023). From 25°C cultures, the supernatants from mid-exponential and late stationary phases demonstrated hemolytic activity to red blood cells (RBCs), above the 75% level by comparison to the expected lysis from the positive control (1% Triton X100) (Figure 1). In contrast, supernatants from *Bc*G9241 grown at 37°C showed very little lytic activity (Figure 1). This led us to the hypothesis that *Bc*G9241 'switches' its phenotype from a hemolytic *B. cereus*-like phenotype at 25°C to a non-hemolytic *B. anthracis*-like phenotype at 37°C.

We expanded the study to test the toxicity of cell free culture supernatants from a range of *Bacillus* cultures grown at 25°C against *ex vivo Manduca sexta* hemocytes. Filtered supernatants were extracted from cultures grown for 16 h. Microscopic examination showed that supernatants from the reference strain *Bc*ATCC14579, *Bc*G9241 and *Bc*G9241 ΔpBCX01 (in which the plasmid had been cured) caused extensive lysis of the *M. sexta* hemocyte (Supplementary Figure S1A). In contrast, supernatants from *B. thuringiensis* 407 Cry-ΔplcR (*Bt ΔplcR*) mutant strain were innocuous, showing no difference from the negative buffer control (Supplementary Figure S1A). *Bt ΔplcR* is an accepted Δ*plcR B. cereus* model as the crystal toxin plasmid has been cured (Lereclus et al., 2000). The cytotoxicity observed with *Bc*G9241 and *Bc*G9241 ΔpBCX01 indicated that cytotoxins were secreted by both strains and

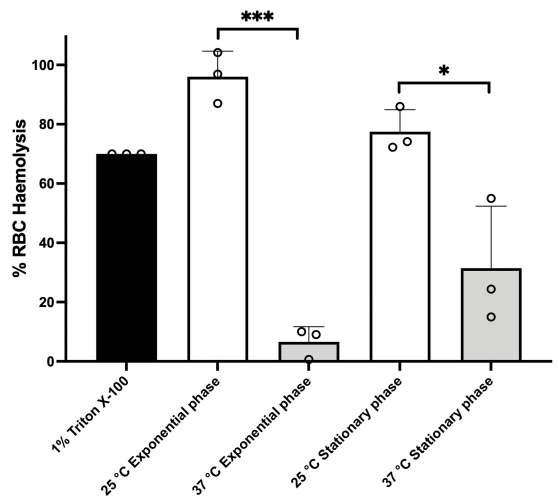

FIGURE 1
*Bc*G9241 supernatant is significantly more toxic to sheep RBCs, when extracted from a 25°C grown culture compared to a 37°C grown culture. The hemolysis assay was conducted by incubating *Bc*G9241 supernatant with 4% RBCs for 1h at 37°C. The OD_{540} was measured, and RBC lysis was calculated as a % of expected RBC lysis by Triton X-100 (1% v/v). Stars above columns represent significance levels: *denotes a value of *p* of 0.0496 and ***denotes a value of *p* of 0.0004 determined by unpaired *t*-test, with Welch's correction. Error bars denote one standard deviation, and all samples were to an *n*=3.

is possibly unaffected by the presence of pBCX01 plasmid at 25°C (Supplementary Figure S1A).

We quantified the effect of supernatants from these same strains using hemocyte cell viability assays. We also expanded the study to include supernatants from the *B. anthracis* Sterne strain, which lacks the pXO2 plasmid (hereon referred to as *Ba* St). Like all *B. anthracis* strains, *Ba* St has a frame-shifted copy of the *plcR* gene. From 25°C grown cultures, we observed cytotoxicity responses consistent with the microscopic examinations (Supplementary Figure S1B), with the supernatants of *Bc*ATCC14579, *Bc*G9241 and *Bc*G9241 ΔpBCX01, all showing potent toxicity. In contrast, supernatants from *Ba* St and *Bt ΔplcR* showed little or no cytotoxicity (Supplementary Figure S1B). However, when grown at 37°C, cytotoxicity of *Bc*G9241 and BcG9241 ΔpBCX01 supernatants was highly attenuated, to levels no different from those of the *Ba* St and *Bt ΔplcR* supernatants (Supplementary Figure S1C). Cytotoxicity of the *Bc*ATCC14579 supernatant was still observed at 37°C (Supplementary Figure S1C). Temperature-dependent cytotoxic activity of *Bc*G9241 and *Bc*G9241 ΔpBCX01 supernatants were also observed in a range of mammalian cells including T2-lymphocytes, polymorphonuclear leukocytes and macrophages (using supernatant extracted from *Bacillus* cultures grown for 16 h), which re-capitulated the trend seen with the insect hemocyte (Supplementary Figure S2).

Temperature and growth phase-dependent proteomic analysis of *Bc*G9241 culture supernatants

In order to investigate the potential cytolytic and hemolytic factors secreted by *Bc*G9241, we analyzed the proteomic profiles of

supernatants from cultures grown at 25°C and 37°C in LB broth, taken from both mid-exponential (OD_{600} = 0.5) and late stationary growth phases. Supernatant was extracted under growth conditions identical to the hemolysis assay shown in Figure 1. Proteins were run through nanoLC-ESI-MS and peptide reads were counted using MaxQuant (Max Planck Institute). Comparisons were made using the Perseus software (Max Planck Institute) and plotted as the difference in proteins expressed between the two temperatures. The full datasets generated can be seen in the Supplementary Datasets S1,S2.

A principal component analysis (PCA) was generated to show the variance between all biological replicates of the *Bc*G9241 supernatants collected from both exponential-and stationary phases. The PCA plots revealed that protein extracts from the exponential phase supernatants overlap with each other, not forming distinct clusters and are highly reproducible (Supplementary Figure S3). The plot also showed that growth temperature affected the protein profiles more significantly at stationary phase compared to exponential phase (Supplementary Figure S3). Furthermore, protein profiles extracted from stationary phase growth at 37°C were more variable than those from other conditions (Supplementary Figure S3).

A diverse and abundant toxin "profile" was secreted at 25°C, while high levels of phage proteins were secreted at 37°C during exponential growth phase of *Bc*G9241

With the cut-off criteria of value of $p < 0.05$ and a minimum 2-fold change in protein level, 33 supernatant proteins were identified as being significantly more abundant at 25°C compared to 37°C. Of these, 11 of the 12 most highly expressed are known toxin homologs (Table 1 and Supplementary Figure S4A). This included all components of the Hbl toxin encoded by the *hbl* operon AQ16_4,930–4,933 (Supplementary Figure S4A-purple arrows). Other known cytotoxic proteins were also abundant in the supernatant at 25°C compared to 37°C, including the Nhe toxin encoded by the *nhe* operon AQ16_658–660 (Supplementary Figure S4A-green arrows), a collagenase (AQ16_1941), a thermolysin metallopeptidase (AQ16_5,317), phospholipase C (Plc, AQ16_1823) and CytK (AQ16_1,392).

Conversely, at 37°C, the secretome contained negligible levels of these cytotoxic proteins (if present at all). There was, however, an abundance of phage capsid proteins encoded by the pBFH_1 phagemid at 37°C compared to 25°C (Supplementary Figure S4A-black arrows). More specifically 25 proteins were found to be more abundant in the secretome at 37°C compared to 25°C. The 10 most abundant proteins at 37°C compared to 25°C were encoded by the pBFH_1 phagemid (Table 1). Proteins from an operon of WxL-domain cell wall-binding proteins were also seen to be more abundant at 37°C compared to 25°C (AQ16_3,217–3,219).

The temperature dependent *Bc*G9241 secretome at late stationary growth phase

Between 25°C and 37°C, 51 proteins showed temperature dependent differences (Table 1; Supplementary Figure S4B). Unlike the mid-exponential observations, the more abundant proteins in the 25°C stationary phase supernatants were not all cytotoxins, although several enzymes were present (Table 1). In fact, of the 11 toxins seen to be more abundant at 25°C during exponential phase growth, only AQ16_5,317 was identified at higher levels at 25°C during stationary phase. This is a thermolysin metallopeptidase, which has a PlcR-box present in the promoter region (Supplementary Table S1), and is over 200-fold more abundant at 25°C compared to 37°C. The relevance of this is discussed below. Several of the more abundant proteins (e.g., AQ16_3,254, 4,226, 374) identified were likely cellular proteins, possibly indicating greater autolysis at 25°C compared to 37°C. The top 5 proteins more abundant in 37°C compared to 25°C supernatants were all extracellular enzymes including two chitinases, a hydrolase, a glucanase and a collagenase (Table 1). In addition, a matrixin family protein (AQ16_4,915), another extracellular enzyme, was also identified as 4.3 log2-fold higher at 37°C. Again, we saw cellular components including 50S ribosome subunit proteins and RecA, which possibly signified cell lysis. Only one of the phage capsid proteins identified as higher at 37°C in the exponential phase secretome, Gp34 (AQ16_5,824), was significantly higher at 37°C in stationary phase.

Temperature-dependent cell proteome analysis of exponentially growing *Bc*G9241 cells

The greatest temperature-dependent change in secreted toxin profiles was seen in exponentially growing cells. Therefore, to investigate the potential role of PlcR in the temperature-dependent regulation of toxin secretion, and any relationship between protein synthesis and secretion, a proteomic analysis of whole cells was performed. The same samples used for the supernatant proteomic analysis were used for this, allowing for direct correlation of the datasets. The full datasets generated can be seen in the Supplementary Dataset S3.

No build-up of toxins was observed in the cellular proteome of *Bc*G9241 at 37°C exponential phase

With a cut-off criteria of value of $p < 0.05$ and a minimum 2-fold change in protein level, 67 proteins were found to be significantly more abundant at 25°C compared to 37°C. The most abundant proteins at 25°C compared to 37°C included cold shock proteins CspA and YdoJ family proteins (Table 2; Supplementary Figure S5). Only two of the toxin proteins seen at higher levels at 25°C in comparison to 37°C in the secretome were also significantly higher in the cell proteome, NheA and NheB (AQ16_659 and 660).

Fifty-one proteins were found to be significantly more abundant at 37°C compared to 25°C (Table 2). Proteins from an operon of WxL-domain cell wall-binding proteins were seen to be more abundant at 37°C (AQ16_3,217–3,219). In addition, various heat stress response proteins were also identified as higher at 37°C. These include: AQ16_3,857, a DNA repair protein; AQ16_512, a DNA protection protein and a thermosensor operon, AQ16_3,712–3,714, involved in protein refolding. Interestingly, despite the significantly increased abundance in the secretome, only two proteins encoded on the pBFH_1 phagemid (AQ16_5,849 and _5858) showed increased abundance in the cell proteome, both of which are uncharacterized.

A build-up of toxins from the cell proteome at 37°C was not observed, demonstrating that temperature-dependent toxin expression is not regulated at the level of secretion. PlcR was detected at both temperatures with no significant difference in abundance levels.

TABLE 1 The 15 most abundant toxins at higher levels at the two temperature in the secretome of *Bc*G9241 during exponential growth and stationary phase.

Log_2-fold change	25°C>37°C at stationary phase	Gene	Gene Loci (AQ16_)
6.46	Hemolysin BL lytic component L2		4,931
5.88	Non-hemolytic enterotoxin binding component	*nheC*	658
5.67	Hemolysin BL-binding component	*hblA*	4,932
4.41	Collagenase family protein		1941
4.31	Extracellular ribonuclease	*bsn*	4,754
3.98	Hemolysin BL-binding component	*hblB*	4,933
3.93	Non-hemolytic enterotoxin lytic component L2	*nheA*	660
3.84	Thermolysin metallopeptidase, catalytic domain protein		5,317
3.77	Non-hemolytic enterotoxin lytic component L1	*nheB*	659
3.57	Hemolysin BL lytic component L1		4,930
3.20	Phospholipase C	*plc*	1823
2.69	Cytotoxin K	*cytK*	1,392
2.49	THUMP domain protein		931
2.44	Probable butyrate kinase	*buk*	3,880
2.42	DEAD-box ATP-dependent RNA helicase	*cshA*	2,258
	37°C>25°C at exponential phase		
5.27	Phage family protein	*gp49*	5,822
4.96	Putative phage major capsid protein	*gp34*	5,824
4.53	Prophage minor structural protein		5,836
4.32	Putative gp14-like protein	*gp14*	5,832
4.31	N-acetylmuramoyl-L-alanine amidase family protein		5,839
3.65	Phage tail family protein		5,835
3.40	Putative major capsid protein	*gpP*	5,831
2.89	Uncharacterized protein		5,823
2.36	WxL domain surface cell wall-binding family protein		3,215
2.34	WxL domain surface cell wall-binding family protein		3,217
2.33	Phage antirepressor KilAC domain protein		5,855
2.30	Dihydropteroate synthase	*folP*	2,448
2.19	Zinc-binding dehydrogenase family protein		318
2.07	WxL domain surface cell wall-binding family protein		3,218
1.95	Toxic anion resistance family protein		2068
	25°C>37°C at stationary phase		
7.83	Thermolysin metallopeptidase, catalytic domain protein		5,317
4.86	Transglutaminase-like superfamily protein		1,487
4.54	UDP-N-acetylglucosamine 1-carboxyvinyltransferase	*murA*	2,685
4.51	Ribonuclease J	*rnjA*	2,375
4.51	Ornithine aminotransferase	*rocD*	1,349
4.16	Pyruvate carboxylase	*pyc*	4,104
4.10	Malic enzyme, NAD binding domain protein		3,400
4.01	CTP synthase	*pyrG*	2,681
3.95	Glycerophosphoryl diester phosphodiesterase family protein		4,572
3.73	Leucine--tRNA ligase	*leuS*	3,254
3.66	Viral enhancin family protein		2,918

(Continued)

TABLE 1 (Continued)

Log_2-fold change	25°C>37°C at stationary phase	Gene	Gene Loci (AQ16_)
3.66	Subtilase family protein		4,301
3.16	50S ribosomal protein L2	*rplB*	2,391
3.16	Aldo/keto reductase family protein		2,308
3.14	Sphingomyelin phosphodiesterase	*sph*	1822
	37°C>25°C at stationary phase		
9.19	Chitinase A1	*chiA1*	2089
7.85	Putative hydrolase		2,662
7.31	Glucanase		5,335
6.99	Collagenase family protein		4,546
5.67	Chitinase A		4,342
4.83	Peptide ABC transporter		2,309
4.54	Calcineurin-like phosphoesterase family protein		4,913
4.43	Urocanate hydratase	*hutU*	4,415
4.31	Single-stranded DNA-binding protein	*ssb*	2,546
4.28	Matrixin family protein		4,915
3.77	3-hydroxyacyl-[acyl-carrier-protein] dehydratase FabZ	*fabZ*	2,750
3.56	Formate acetyltransferase	*pflB*	2025
3.52	Ribose-phosphate pyrophosphokinase	*prs*	2,472
3.26	Putative phage major capsid protein		5,824
3.22	50S ribosomal protein L4	*rplD*	2,393

The significance cut-off criteria used was a value of p of <0.05 and a minimum of a 2-fold change in protein level.

Analysis of PlcR-controlled toxin expression in *Bc*G9241

Hemolytic and cytolytic assays have suggested that *Bc*G9241 containing a functional copy of the *plcR* gene show temperature-dependent toxicity. Hbl, Nhe, Plc, CytK, and a thermolysin metallopeptidase (AQ16_5,317), which are regulated by the PlcR-PapR circuit (Gohar et al., 2008), were detected with high abundance in the secretome analysis at 25°C compared to 37°C. In order to confirm the temperature-dependent toxin and protease production, a panel of transcription-translation reporter plasmids were made, in which the promoter regions and the first 24 bp of the coding sequence of *hblC, nheA, plc, cytK*, and *AQ16_5,317* (which includes the start codon) were genetically fused in frame to a *gfp* gene, excluding the start codon of the reporter gene (referred to hereon as *hblC::gfp, nheA::gfp, plc::gfp, cytK::gfp*, and *AQ16_5,317::gfp*). Note that only eight N-terminal amino acids from the ORF were cloned as it is not sufficient to serve as a Sec-dependant secretion signal for the toxins, preventing the GFP from being secreted. For comparison, GFP reporters of PlcR-regulated toxins were also constructed for *Bc*ATCC14579 from homologous regions. Each of the reporter constructs were then transformed into the relevant *B. cereus* strain and examined using fluorescence microscopy and microtitre plate reader assays to assess the expression patterns across growth phases at 25°C and 37°C, when grown in LB while maintaining plasmid marker selection. The rate of change in fluorescence ($\Delta GFP/OD_{600}$) was calculated every hour by subtracting the fluorescence at a given time point by the fluorescence of the previous time point. This would reveal when the biggest change in GFP expression occurs across the growth phase.

From the microscopy images, the expression of the toxin reporters in *Bc*G9241 was not detected during mid-exponential phase at 25°C and 37°C (Figure 2A; Supplementary Figure S6). However, by quantifying the GFP intensity of *B. cereus* strains containing the reporters, there were cells with higher fluorescence compared to the control cells (being above the threshold), suggesting that GFP, and therefore the PlcR-regulated proteins were being expressed. The mean GFP intensity of individual cells quantified was higher at 25°C compared to 37°C for *hblC::gfp*, *nheA::gfp* and *cytK::gfp* (Supplementary Figure S7). Once reaching early stationary phase (Supplementary Figure S8), the difference in the expression of the toxin reporters in *Bc*G9241 was more pronounced between 25°C and 37°C (Figure 2A; Supplementary Figure S6). From GFP intensity quantification of individual cells from the micrographs, the mean GFP intensity of *hblC::gfp, nheA::gfp, plc::gfp* and *AQ16_5,317::gfp* at the onset of stationary phase and 24 h was higher at 25°C compared to 37°C in *Bc*G9241 (Supplementary Figure S7). It is interesting to note that *Bc*G9241 cells formed filamentous-like structures during exponential phase which reverted to shorter vegetative rod morphologies once stationary phase was reached.

When the GFP intensity/OD_{600} of *Bc*G9241 harboring the PlcR-regulated toxin reporters was monitored with a microtitre plate reader over 24 h (Figure 2B; Supplementary Figure S6), the GFP expression was greater at 25°C compared to 37°C for *hblC::gfp, nheA::gfp, plc::gfp* and *AQ16_5,317::gfp* while the expression of *cytK::gfp* appeared similar between both

TABLE 2 Top 15 cellular proteins that are more abundant at each temperature in exponentially growing *Bc*G9241.

Log_2-fold change	25°C>37°C at exponential phase	Gene	Gene Loci (AQ16_)
5.09	Major cold shock protein	*cspA*	1,368
4.72	Uncharacterized protein		4,251
4.48	Cold-inducible YdjO family protein		175
4.10	Uncharacterized protein		4,821
3.18	Transglutaminase-like superfamily protein		1,487
3.06	Flagellar motor switch FliM family protein		858
2.77	FMN-dependent NADH-azoreductase	*azoR4*	2,611
2.57	Uncharacterized protein		1,372
2.47	Hemolytic enterotoxin family protein		659
2.41	Uncharacterized protein		1,559
2.21	Major cold shock protein	*cspA*	174
2.20	SET domain protein		2,908
2.19	Transposase family protein		1725 / 4,355
2.15	Rhodanese-like domain protein		1704
2.09	Hemolytic enterotoxin family protein	*nheA*	660
	37°C>25°C at exponential phase		
4.34	WxL domain surface cell wall-binding family protein		3,218
3.74	Uncharacterized protein		3,219
2.87	Formate acetyltransferase	*pflB*	2025
2.73	Uncharacterized protein		1,429
2.29	DNA repair protein	*recN*	3,857
2.27	DNA protection during starvation protein 1	*dps1*	512
2.25	Uncharacterized protein		5,765
2.25	Pyruvate formate-lyase-activating enzyme	*pflA*	2024
2.23	L-lactate dehydrogenase	*ldh*	3,111
2.166	CamS sex pheromone cAM373 family protein		2,171
2.09	L-asparaginase, type I family protein		4,939
1.98	Heat-inducible transcription repressor	*hrcA*	3,712
1.97	Uncharacterized protein		5,849
1.96	Membrane MotB of proton-channel complex MotA/MotB family protein		3,490
1.84	Periplasmic binding family protein		1888

The significance cut-off criteria used was a value of p of <0.05 and a minimum 2-fold change in protein level.

temperatures. By calculating the rate of change in fluorescence (ΔGFP), a large and broad ΔGFP peak was observed at 25°C while the peak appeared tighter at 37°C for *hblC::gfp, nheA::gfp, plc::gfp* and *AQ16_5,317::gfp* (Supplementary Figure S9). In comparison, expression of *hblC::gfp*, *nheA::gfp* and *BC_2735::gfp* (BC_2735 has a 97% identity to AQ16_5,317 using BLASTP) in *Bc*ATCC14579 appeared to be similar at 25°C and 37°C, while the expression of *plc::gfp* and *cytK::gfp* was temperature-dependent (Supplementary Figure S10).

Population level analysis of PlcR and PapR expression in *Bc*G9241

Subsequently, we expanded the analysis by including a panel of transcription-translation reporter plasmids for PlcR and PapR in *Bc*G9241 and *Bc*ATCC14579. The promoter regions and the first 24 bp of the coding sequence of *plcR* and *papR* (including the start codon) were genetically fused in frame to a *gfp* gene, while excluding the start codon of the reporter gene (referred to hereon as *plcR::gfp* and *papR::gfp*). Note that only eight N-terminal amino acids from the ORF were cloned as it is not sufficient to serve as a Sec-dependent secretion signal for PapR and to make sure that the PlcR protein was not interfering with the GFP protein. Each of the reporter constructs were then transformed into the relevant *B. cereus* strain and examined using fluorescence microscopy to assess the expression patterns across growth phases at 25°C and 37°C, when grown in LB and maintaining plasmid marker selection.

Expression of PlcR is not temperature dependent

Expression of *plcR::gfp* was first observed during early stationary phase at 25°C and 37°C (Figure 3A). By 24 h, levels of *plcR::gfp*

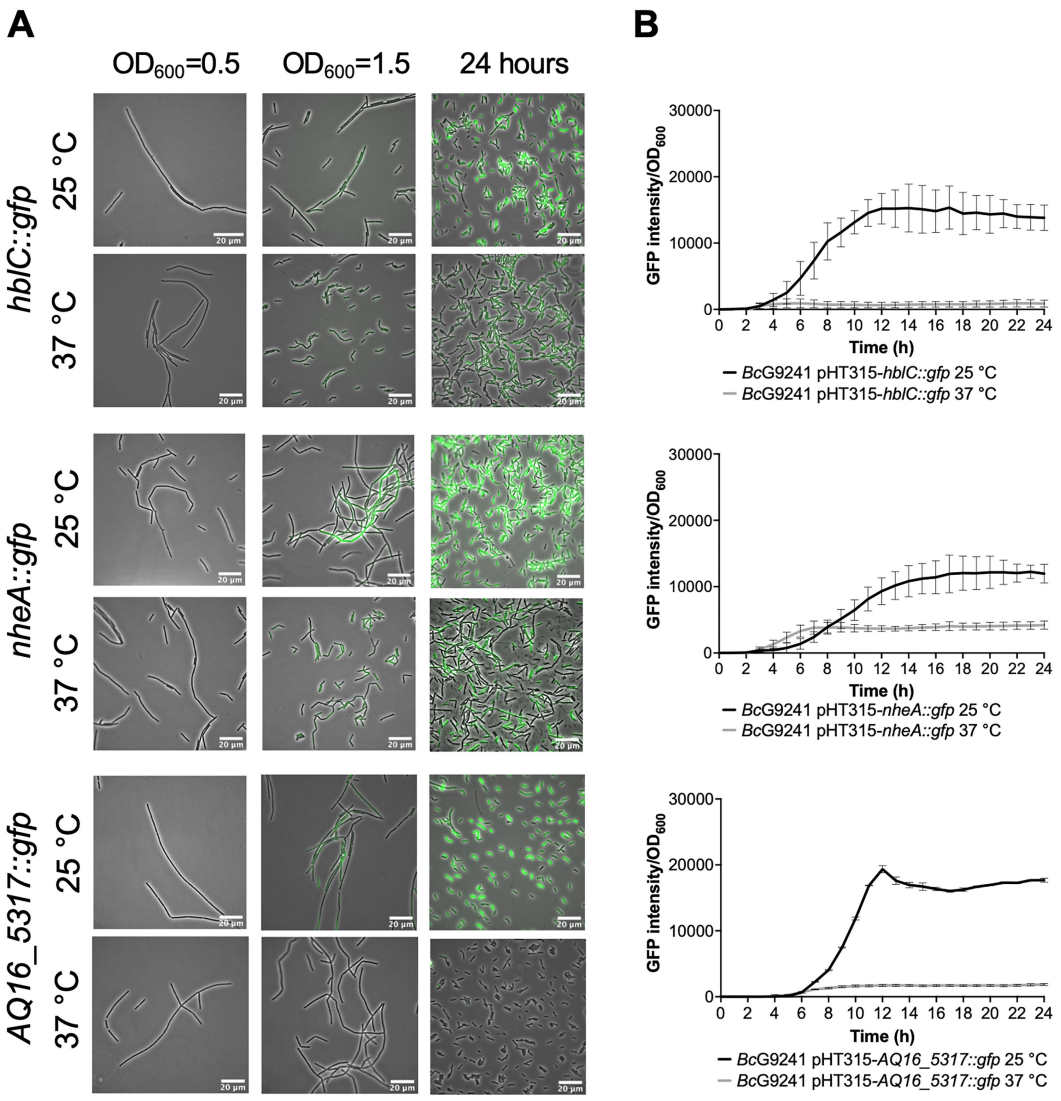

FIGURE 2
Temperature dependent expression of PlcR-regulated toxins and enzymes in *Bc*G9241 using GFP reporters. **(A)** A representative selection of microscopy images of the plasmid-based transcription-translation GFP reporters of PlcR-regulated toxins for *Bc*G9241 taken at three different time points: mid-exponential phase which is 2h at 37°C and 5h at 25°C (OD_{600}=0.5), early stationary phase which is 4h at 37°C and 7h at 25°C (OD_{600}=1.5) and 24h. Scale bar=20 μm. **(B)** Fluorescence of toxin reporters over time in LB. GFP intensity/OD_{600} and change in GFP (ΔGFP/OD_{600}) of *Bc*G9241 containing PlcR-regulated toxin reporters over 24h growth in 100μL volume LB media at 25°C (in black) and 37°C (in gray). Each line represents the mean of three biological replicates with three technical replicates each and error bars denote standard deviation.

increased at both temperatures, with a high level of population heterogeneity in expression within the cell population. The cells that expressed *plcR::gfp*, also did so at a high level. As observed in *Bc*G9241, expression of *plcR::gfp* in *Bc*ATCC14579 was also heterogeneous within the cell population (Figure 3A). Image analysis provided an objective quantification of this heterogeneous expression observed within the cell population, with a small number of cells expressing *plcR::gfp* in both *B. cereus* strains (Supplementary Figure S11).

There is a possibility that the population heterogeneity observed for the expression of *plcR::gfp* could be due to cell death or an error from the reporter itself. To determine whether the *plcR::gfp* expression was indeed originated from a minority of cells, some potential issues were analyzed. The high-copy shuttle vector used for the reporter pHT315 encodes an erythromycin resistance gene, and therefore the antibiotic was added to maintain selection. To rule out heterogeneity due to cell death, propidium iodide staining was carried out. Cell viability is assessed when propidium iodide penetrates damaged membranes binding to nucleic acid, leading to fluorescence. At early stationary phase, only a few cells were stained by propidium iodide while within a large population of live cells, a small proportion of cells expressed *plcR::gfp* (Supplementary Figure S12). This confirms the heterogeneous expression of *plcR::gfp* was indeed originated from a small subpopulation of live cells and this is not a consequence of cell death in any non-reporter expressing cells.

PapR in *Bc*G9241 is highly expressed at 37°C compared to 25°C

Expression of *papR::gfp* was first noticed during early stationary phase at 25°C and 37°C. Levels of *papR::gfp* expression greatly increased by 24 h, with stronger fluorescence observed by microscopy

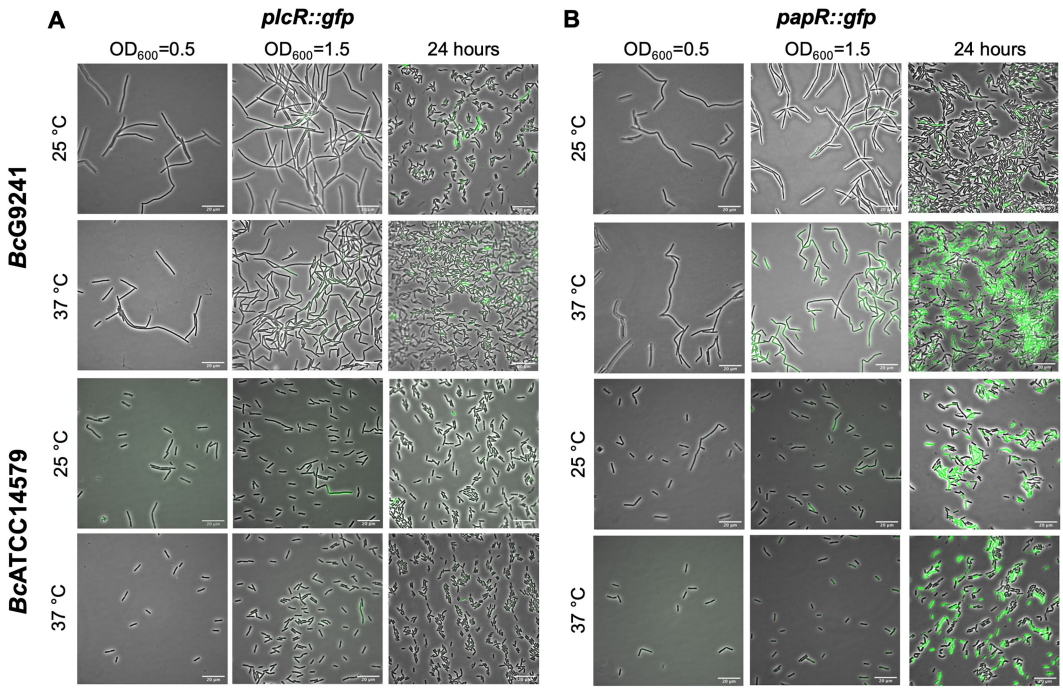

FIGURE 3
A representative selection of microscopy images of *Bc*G9241 and *Bc*ATCC14579 harboring the transcription-translation GFP reporters of *plcR::gfp* and *papR::gfp*. Micrographs of strains harboring **(A)** *plcR::gfp* and **(B)** *papR::gfp* were taken at three different time points: mid-exponential phase which is 2h at 37°C and 5h at 25°C (OD_{600}=0.5), early stationary phase which is 4h at 37°C and 7h at 25°C (OD_{600}=1.5) and 24h. Scale bar=20 μm.

at 37°C compared to 25°C (Figure 3B). Image analysis has provided an assessment of the expression observed within the cell population, with a sub-population of cells expressing *papR::gfp* at 25°C. In *Bc*G9241 and *Bc*ATCC14579, the mean GFP expression was higher at 37°C compared to 25°C (Supplementary Figure S11).

The import of mature $PapR_7$ is functional at 25°C and 37°C in *Bc*G9241

A build-up of toxin proteins in the cell proteome at 37°C was not detected, suggesting that temperature-dependent toxin expression is not regulated at the level of secretion. This led us to investigate whether the import of mature PapR is not functional at 37°C, causing the temperature-dependent hemolysis and cytolysis phenotypes observed in *Bc*G9241. To understand whether the import system is functional at 37°C, a hemolysis assay was carried out using supernatants of *B. cereus* cultures extracted at mid-exponential and early stationary phase (Supplementary Figure S8) and grown at 25°C and 37°C, with mature synthetic PapR peptides added exogenously. Note that supernatant at early stationary phase was used as the expression of *plcR* using the plasmid-based transcription-translation GFP reporter was first observed at the onset of stationary phase (Figure 3). Previous studies have demonstrated that the heptapeptide $PapR_7$ is the mature form of the quorum sensing peptide (Slamti and Lereclus, 2005; Pomerantsev et al., 2009) and therefore synthetic peptides of this form (G9241 $PapR_7$ = SDLPFEH, ATCC14579 $PapR_7$ = KDLPFEY) were used.

At 25°C, with the addition of exogenous self $PapR_7$ (i.e., adding G9241 $PapR_7$ into cultures of *Bc*G9241 or adding ATCC14579 $PapR_7$ into cultures of *Bc*ATCC14579), no significant change in hemolytic activity of the mid-exponential supernatants of *Bc*G9241 was observed, compared to the absence of exogenous $PapR_7$. Nevertheless, hemolytic activity was still observed with/without the addition of the cognate $PapR_7$ from supernatants collected at 25°C in both *Bc*G9241 and *Bc*ATCC14579 (Figure 4). In comparison, upon the addition of exogenous PapR a significant change in hemolytic activity of the mid-exponential supernatant of *Bc*ATCC14579 was observed, compared to the absence of exogenous $PapR_7$. At 37°C, with the addition of cognate $PapR_7$, there was a significant increase in hemolytic activity with the mid-exponential and early stationary phase *Bc*G9241 supernatant (Figure 4). This suggests that $PapR_7$ can get taken into the cell through an import system at 37°C. In comparison, upon the addition of exogenous cognate $PapR_7$, no significant change in hemolytic activity of the mid-exponential supernatant of *Bc*ATCC14579 was observed, compared to the absence of exogenous $PapR_7$.

Addition of exogenous non-self $PapR_7$ molecules in *Bc*G9241 and *Bc*ATCC14579 (i.e., adding G9241 $PapR_7$ into cultures of *Bc*ATCC14579 or adding ATCC14579 $PapR_7$ into cultures of *Bc*G9241) led to a decrease in hemolytic activity at both temperatures (Figure 4). This implies that the correct $PapR_7$ is required for the expression of toxins, and that a non-self cognate variant of the peptide can actually interfere with the native PlcR-PapR circuit.

Subsequently, we wanted to observe how the addition of the synthetic $PapR_7$ would affect the expression of PlcR-regulated toxins in *Bc*G9241 at 37°C using the plasmid-based GFP reporters we have

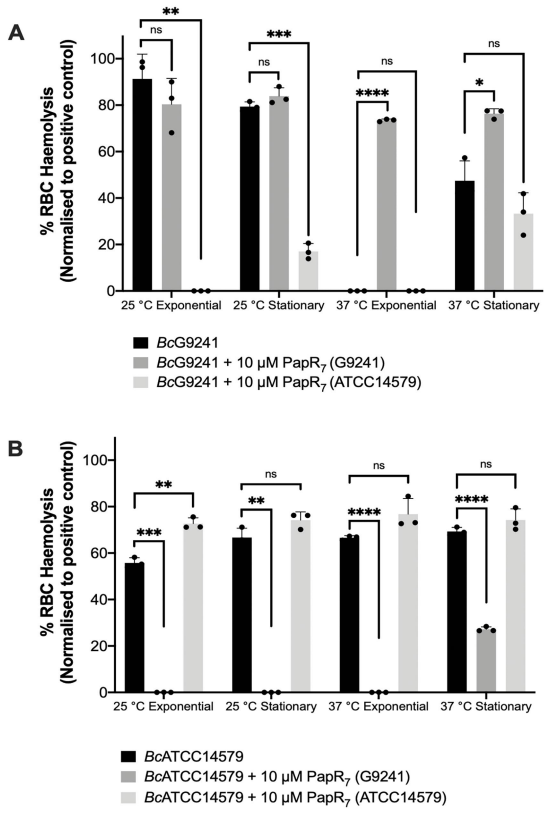

FIGURE 4
The effect of exogenous $PapR_7$ in *Bc*G9241 and *Bc*ATCC14579. 10 µM synthetic $PapR_7$ (G9241 $PapR_7$=SDLPFEH, ATCC14579 $PapR_7$=KDLPFEY) were added when the bacterial culture was inoculated from OD_{600}=0.005. Supernatant was extracted from mid-exponential and early stationary phase growing **(A)** *Bc*G9241 and **(B)** *Bc*ATCC14685. Supernatant was filter-sterilized and incubated with 4% RBCs for 1h. OD_{540} was measured and RBC lysis was calculated as a percentage of expected RBC lysis, normalized with 70% lysis from 1% (w/w) Triton X-100. Error bars denote one standard deviation, and all samples were to an n=3. * [p<0.05], **[p<0.01], ***[p<0.001], and ****[p<0.0001] as determined by unpaired t-test, with Welch's correction.

available. At 25°C, addition of the cognate $PapR_7$ to *Bc*G9241 led to a slight increase in expression of *nheA::gfp*, no change in expression of *plc::gfp* and *cytK::gfp* and a decrease in expression of *hblC::gfp*. A decrease in the expression of *hblC::gfp* was still observed when lower concentrations of synthetic PapR were added to *Bc*G9241 cultures (data not shown). At 37°C, addition of cognate $PapR_7$ to *Bc*G9241 led to a dramatic increase in expression of Nhe, Plc and CytK. This suggests that the processed PapR can indeed get imported into cells at 37°C. There is no significant increase in *hbl::gfp* expression with the addition of $PapR_7$ at 37°C (Supplementary Figure S13) suggesting an additional level of regulation for these genes.

The PapR maturation process is potentially preventing the expression of PlcR-controlled toxins in *Bc*G9241 at 37°C

The import of mature PapR does not appear to be a limiting factor involved in the temperature-dependent toxin expression phenotype. Consequently, there is a possibility that the protease(s) involved in processing PapR represents the limiting step within the PlcR-PapR circuit in *Bc*G9241. In *B. cereus* 569, it has been shown that the neutral protease NprB is involved in processing the pro-peptide $PapR_{48}$ into the shorter and active form $PapR_7$ (Pomerantsev et al., 2009). In some *B. cereus* and *B. thuringiensis* genomes, the gene *nprB* is found adjacent to *plcR* and transcribed in the opposite orientation (Lereclus et al., 1996; Økstad et al., 1999; Pomerantsev et al., 2009). To identify whether *Bc*G9241 and other *B. cereus-B. anthracis* "cross-over" strains have a functional copy of *nprB*, a synteny analysis using SyntTax[1] was carried out. SyntTax uses the genomic and taxonomic database obtained from NCBI. The NprB protein sequence from *Bc*ATCC14579 (RefSeq accession GCF_000007835.1) was used as the query protein. As shown in Figure 5, *Bc*G9241 as well as the "cross-over" strains *B. cereus* 03BB87, *B. cereus* 03BB102, *B. cereus* BC-AK and *B. cereus* bv *anthracis* CI can be seen to encode only remnants of the *nprB* gene located near the *plcR-papR* operon, with low synteny scores. In comparison, some *B. cereus sensu stricto* and *B. thuringiensis* strains have intact copies of *nprB*, as previously described (Lereclus et al., 1996; Økstad et al., 1999; Pomerantsev et al., 2009) with synteny scores above 97% (Figure 5). *B. anthracis* strains (Ames and Sterne) also lack the full copy of the *nprB* gene (Pomerantsev et al., 2009). This indicates that NprB may not be involved in processing PapR in *B. cereus* strains carrying functional copies of both *plcR* and *atxA*.

This led us to question which protease(s) is/are capable of processing PapR in *Bc*G9241 and whether the temperature-dependent toxin expression in *Bc*G9241 is due to differential expression of these theoretical alternative protease enzymes. From the *Bc*G9241 secretome analysis of the supernatant extracted from cultures grown at 25°C and 37°C, several proteases were identified as highly expressed at 25°C compared to 37°C that could potentially be involved in processing PapR in *Bc*G9241 to its active form (Table 1). To determine whether temperature-dependent proteolytic activity is present in *Bc*G9241 as suggested by the secretome analysis, a protease activity assay was carried out using skim milk agar plates. Filtered supernatant of *Bc*G9241 grown at mid-exponential phase 25°C showed hydrolysis of the skimmed milk casein whereas no clear zone was observed from cultures grown at mid-exponential phase 37°C, which demonstrates that there is indeed a temperature-dependent protease activity deployed during mid-exponential phase of growth (Supplementary Figure S14). Supernatants of *B. cereus* cultures into which synthetic $PapR_7$ was added were also collected and spotted onto skim milk agar to look for any changes in proteolytic activity. Interestingly, the addition of the synthetic $PapR_7$ peptide to cultures of either *Bc*G9241 or *Bc*G9241 ΔpBCX01 led to a significant increase in proteolytic activity at both temperatures (Supplementary Figure S14), presumably caused by PlcR-regulated proteases such as the thermolysin metallopeptidase (AQ16_5,317), which we have shown to be highly expressed at 25°C compared to 37°C (see above).

From the secretome analysis, AQ16_5,317 labeled as a thermolysin metallopeptidase was found to be highly abundant at 25°C compared to 37°C during mid-exponential and late stationary phase (Table 1). Out of all these proteases/enzymes listed in Table 1, only the gene encoding the thermolysin metallopeptidase and

1 https://archaea.i2bc.paris-saclay.fr/SyntTax/Default.aspx

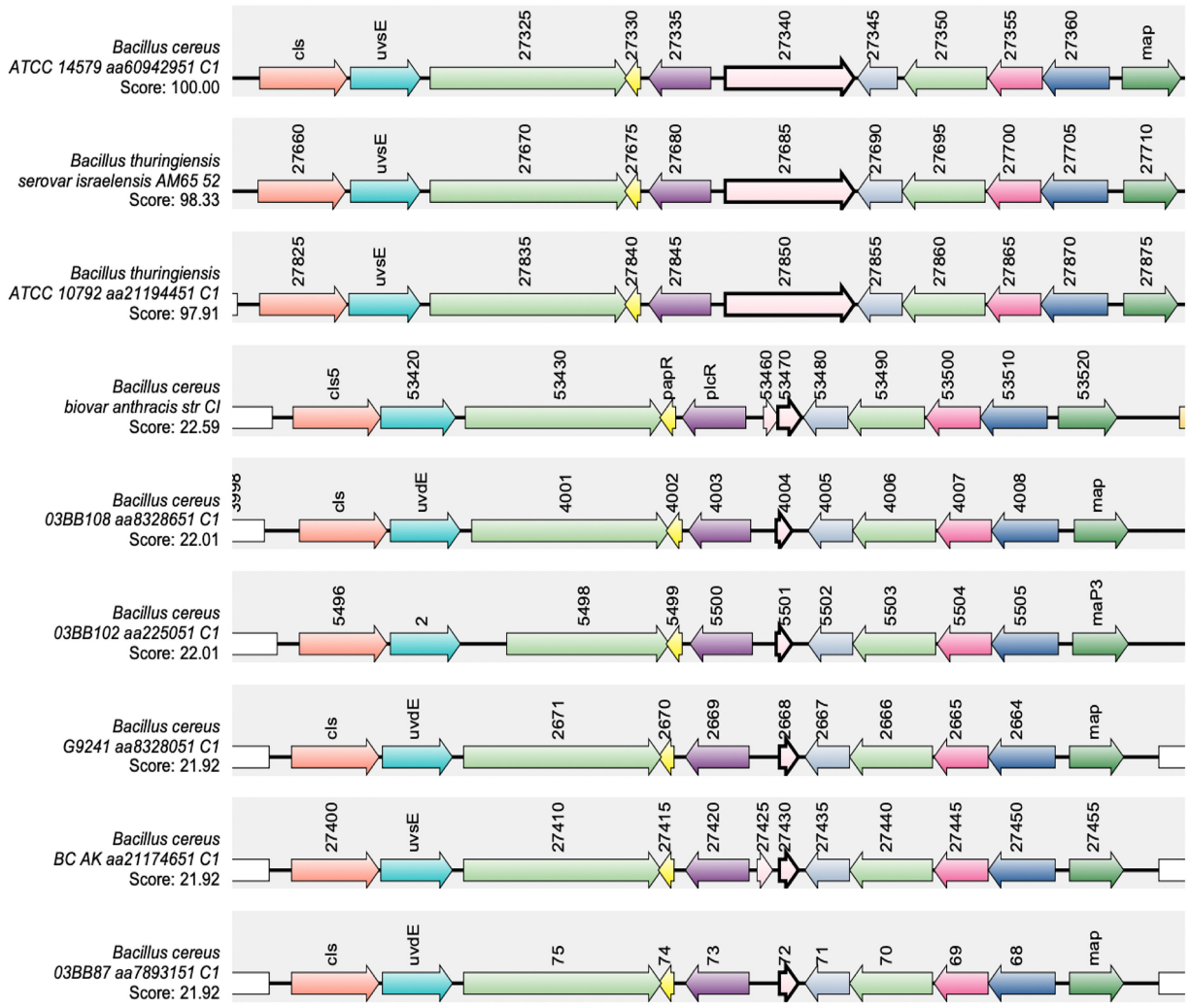

FIGURE 5
Synteny of the gene encoding *nprB* in *B. cereus sensu stricto, B. thuringiensis, B. cereus* "cross-over" strains and *B. anthracis*. The NprB protein sequence from *Bc*ATCC14579 (RefSeq accession GCF_000007835.1) was used as the query protein. The gene encoding *nprB* is shown in pink with a bold border, *plcR* and *papR* are shown in purple and yellow, respectively. SynTax, a synteny web service, was used to look in the conservation of gene order (https://archaea.i2bc.paris-saclay.fr/SyntTax/Default.aspx).

collagenase has a PlcR-box on the promoter region. There is a possibility that AQ16_5,317 is a protease involved in processing PapR in *Bc*G9241. From a synteny analysis to look into whether AQ16_5,317 thermolysin metallopeptidase was present in other *B. cereus* species, a high synteny score was shown in some of the *B. cereus-B. anthracis* "cross-over" strains, as well as *B. cereus sensu stricto*, *Bacillus weihenstephanensis, B. anthracis* and *B. thuringiensis* (Supplementary Figure S15).

To identify whether expressing AQ16_5,317 at 37°C would abolish the temperature-dependent hemolytic phenotype, the AQ16_5,317 ORF with a promoter not linked to the PlcR-PapR regulator (*fusA* promoter) was cloned into the shuttle vector pHT315 which should be able to constitutively express the protease. When measuring the OD_{600} over 24 h using a microplate reader, strains containing the pHT315-*fusA*$_p$-*AQ16_5,317* construct did not alter the growth of the bacteria (Supplementary Figure S16). A hemolysis assay using sheep erythrocytes was carried out with *Bc*G9241 strains containing the constitutively expressed AQ16_5,317. Cell free culture supernatants from cultures grown at 25°C and 37°C from mid-exponential and early stationary phase were tested in this assay. Supernatants from 25°C mid-exponential and early stationary phase cultures showed no change in hemolytic activity, with or without the constitutive expression of *AQ16_5,317*. However, at 37°C mid-exponential phase, constitutive expression of AQ16_5,317 expressed at 37°C led to a significant increase in hemolytic activity compared to the control (Figure 6). This result suggests that this protease is capable of processing PapR at 37°C, leading to the increased expression of the PlcR regulon. Supernatants from 37°C early stationary phase cultures displayed hemolytic activity, with or without the constitutive expression of *AQ16_5,317,* though there was no significant change between the two conditions. This is a contrast to what is observed in Figure 4, where the supernatants from 37°C early stationary phase cultures did not display a high hemolytic activity. It is possible that the presence of the *fusA* promoter on a high copy number plasmid may have affected the normal biological processes and regulation of the cell.

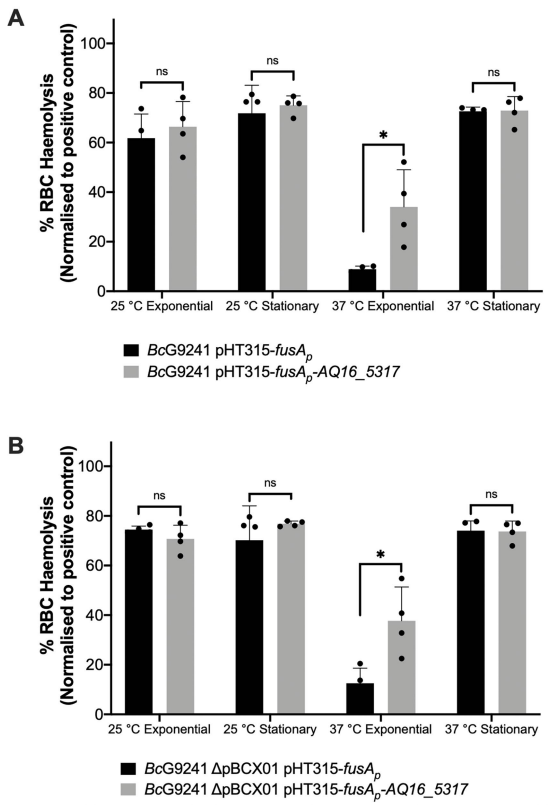

FIGURE 6
Slight increase in hemolytic activity with the presence of AQ16_5,317 at 37°C during exponential phase. The hemolysis assay was conducted by incubating the supernatant extracted from mid-exponential and early stationary phase of **(A)** *Bc*G9241 and **(B)** *Bc*G9241 ΔpBCX01 with 4% RBC for 1 h at 37°C. OD_{540} was measured and RBC lysis was calculated as a percentage of expected RBC lysis, normalized with 70% lysis from 1% (w/w) Triton X-100. Stars above columns represent significance levels: * [$p<0.05$] as determined by unpaired *t*-test, with Welch's correction. Error bars denote one standard deviation, and all samples were to an $n=4$.

Discussion

The roles and expression of PlcR and AtxA are relatively well defined in *B. cereus* and *B. anthracis,* respectively. In *B. anthracis*, AtxA transcription and accumulation are enhanced at 37°C compared to 28°C (Dai and Koehler, 1997). In *B. cereus* and *B. thuringiensis*, PlcR transcription has been observed at the onset of stationary phase, suggesting cell density is required for transcription of the regulon (Lereclus et al., 1996; Brillard et al., 2008). Also, the *B. weihenstephanensis* KBAB4 is reported to exhibit temperature-dependent production of PlcR and PlcR-regulated toxins (Réjasse et al., 2012). However, due to the rare nature of some *B. cereus* strains containing both *plcR* and *atxA* (Hoffmaster et al., 2004, 2006; Sue et al., 2006; Avashia et al., 2007; Wright et al., 2011; Marston et al., 2016; Pena-Gonzalez et al., 2017), the understanding of how a bacterium such as *Bc*G9241 has incorporated two hypothetically conflicting virulence regulators (Mignot et al., 2001) has not yet been studied in detail.

Hemolysis and cytolysis assays using the supernatant of *Bc*G9241 collected at 16 h demonstrated lytic activity at 25°C but not at 37°C. The supernatant of *Bc*G9241 ΔpBCX01 collected at 16 h also demonstrated temperature-dependent hemolytic and cytolytic activity, suggesting that this phenotype is not dependent on the pBCX01 virulence plasmid encoding AtxA1. In comparison, the supernatant of *Bt* Cry-ΔplcR and *Ba St* collected at 16 h showed little or no cytotoxicity against a variety of eukaryotic cells at both temperatures. As *Bt* Cry-ΔplcR and *Ba St* lack a functional *plcR* gene, it supports the hemolysis that PlcR-regulated toxins are responsible. It should be noted that as the supernatants were collected at 16 h, the temperature dependent phenotype observed in *Bc*G9241 strains could have been due to the strains already engaging in the sporulation process at 37°C. As PlcR is under the control of Spo0A, Spo0A ~ P is able to inhibit the expression of PlcR and in turn does not express the toxins. Therefore, another hemolysis assay using the supernatant of *Bc*G9241 collected at mid-exponential and late stationary phase (with the bacteria being under vegetative state) was also carried out, which has also demonstrated a higher lytic activity at 25°C in comparison to 37°C. Together these findings led us to propose that *Bc*G9241 'switches' its phenotype from a hemolytic *B. cereus*-like phenotype at 25°C to a non-hemolytic *B. anthracis*-like phenotype at 37°C.

The differential cytotoxicity pattern appears to be caused by the secretion of multiple cytolytic and hemolytic toxins at 25°C, which includes Hbl, Nhe, Plc, CytK, and a thermolysin metallopeptidase encoded by AQ16_5,317, detected from the secretome analysis of exponentially grown *Bc*G9241 cells. The corresponding genes for these toxins and enzymes are preceded by a PlcR box sequence (Supplementary Table S1) and are known to be transcriptionally regulated by PlcR in *Bc*ATCC14579 (Agaisse et al., 1999; Lereclus et al., 2000). Using a plasmid-based transcription-translation GFP reporters, we were able to confirm that *hblC::gfp, nheA::gfp, plc::gfp* and *AQ16_5,317::gfp* are expressed in a temperature dependent manner, with higher expression at 25°C in *Bc*G9241. This was also observed in *Bc*G9241 ΔpBCX01 (data not shown), further confirming that the temperature-dependent toxin production is independent of the virulence plasmid. In contrast, the expression of *hblC::gfp, nheA::gfp*, and *BC_2735::gfp* in the *B. cereus* type strain *Bc*ATCC14579 were at a similar level between the two temperatures. Expression of *cytK::gfp* in *Bc*G9241 was heterogeneous within the cell population, which Ceuppens et al. (2012) also observed in *Bc*ATCC14579 using a plasmid-based cyan fluorescent protein reporter (Ceuppens et al., 2012).

Interestingly, the most abundant proteins from the secretome analysis at 37°C were phage proteins from the pBFH_1 phagemid. This is in agreement with the transcriptomic data carried out by our group (Taylor-Joyce et al., 2023), where high transcript levels of genes encoded on the pBFH_1 phagemid were identified at 37°C compared to 25°C from mid-exponentially grown *Bc*G9241 cells. However, at this stage we have not confirmed whether phage protein expression is the cause or the effect of a loss of PlcR-mediated toxin expression at 37°C, or indeed entirely independent.

The cell proteome analysis of mid-exponentially grown *Bc*G9241 cells revealed no accumulation of toxins at 37°C, implying that temperature-dependent toxin expression is not regulated at the level of secretion. Also, PlcR was detected at both temperatures from the cell proteome analysis with no significant difference between expression levels.

In *Bc*G9241 and *Bc*ATCC14579, expression of PlcR using a plasmid-based transcription-translation GFP reporters was first

observed at the onset of stationary phase, in agreement with previous observations in *B. thuringiensis* (Lereclus et al., 1996). Expression of PlcR was highly heterogeneous during the onset of stationary phase and by 24 h. As PlcR is under the direct-and indirect influence of other transcriptional regulators such as Spo0A and CodY (Lereclus et al., 2000; Slamti et al., 2016), it is possible that these regulators play a role in the heterogeneous expression of PlcR. Spo0A ~ P is able to inhibit the expression of PlcR due to the presence of two Spo0A-boxes between the PlcR box in the promoter region of *plcR* (Lereclus et al., 2000), while CodY controls the Opp system involved in importing processed PapR into the cell to activate PlcR (Slamti et al., 2016). Population heterogeneity between genetically identical cells could be beneficial in order to survive, persist in fluctuating environment or be helpful for division of labor between cells. We have ruled out that the heterogeneity observed from the expression of *plcR* is not due to cell death. However, there is still a possibility that the heterogeneity of the *plcR* expression in some bacterial cells is due to the high copy number of the plasmid vector. The *plcR* gene is known to be expressed at a low level (Lereclus et al., 1996) and the use of the high-copy shuttle vector pHT315 may have resulted in an unusually high level of *plcR* expression in a few bacterial cells. Transcription-translation expression of PapR using GFP reporters was also observed across the growth phase. Unexpectedly, expression of PapR in *Bc*G9241 increased dramatically at 37°C, with a near homogenous expression observed by 24 h. This is in contrast with what is observed in *Bc*ATCC14579, where the expression of PapR was heterogeneous at 25°C and 37°C.

As the analysis of the cell proteome did not show a build-up of toxins at 37°C, we wanted to identify whether the temperature-dependent toxin production was caused by a limiting step within the PlcR-PapR regulatory circuit in *Bc*G9241: import of mature PapR or processing of immature PapR.

Addition of synthetic $PapR_7$ to *Bc*G9241, which would bypass the secretion and processing of the full-length peptide restored hemolytic activity at 37°C. Supplementing the non-cognate form of the $PapR_7$ peptide into *B. cereus* strains led to suppression of hemolytic activity at both temperatures, confirming that the activating mechanism of PlcR-PapR is strain specific. This observation has been previously noted in *B. thuringiensis* (Slamti and Lereclus, 2005). Using the PlcR-regulated toxin reporter strains made in this study, the addition of synthetic $PapR_7$ led to an increase in *nheA::gfp, plc::gfp* and *cytK::gfp* expression at 37°C in *Bc*G9241. This confirms that the mature form of PapR can be imported into the cell at 37°C in order to bind to PlcR and express the PlcR regulon. Also, as Nhe is a known hemolysin that causes lytic activity on erythrocytes (Fagerlund et al., 2008), the increased expression of *nheA::gfp* seen under the same conditions potentially correlates with the increased hemolytic activity of *Bc*G9241 observed in Figure 4. Intriguingly, there was no significant increase in *hblC::gfp* expression at 37°C with the addition of $PapR_7$, while the addition of $PapR_7$ at 25°C led to a decrease in the expression of *hbl::gfp* in *Bc*G9241. There is a possibility that there are other regulators that play a role in the expression of this enterotoxin such as ResDE (redox regulator), FnR, RpoN, and Rex (Duport et al., 2006; Zigha et al., 2007). It has been demonstrated that FnR, ResD and PlcR are able to form a ternary complex *in vivo* (Esbelin et al., 2012), which could explain the decrease of Hbl expression when synthetic $PapR_7$ were added. However, further experimental analysis would be required to understand the role of these regulators potentially affecting the expression of the *hbl* operon in *Bc*G9241.

Finally, this led us to question as to whether the processing of PapR by an extracellular protease(s) was the limiting step causing the temperature-dependent toxin expression. The gene *nprB*, which encodes for a neutral protease involved in processing PapR in some *B. cereus* and *B. thuringiensis* strains is truncated in *B. anthracis* (Pomerantsev et al., 2009), as well as in *Bc*G9241 and some of the *B. cereus-B. anthracis* "cross-over" strains that carry functional copies of *plcR-papR* and *atxA* (Hoffmaster et al., 2004, 2006; Sue et al., 2006; Avashia et al., 2007; Wright et al., 2011; Marston et al., 2016; Pena-Gonzalez et al., 2017). The loss of a functional copy of *nprB* may have contributed to the accommodation of *atxA* in these strains and potentially allowed *B. cereus-B. anthracis* "cross-over" strains to carry both regulators. Interestingly there are *B. cereus* strains such as ATCC 10987, the emetic strain AH87 (accession number CP001177.1) and NVH 0075–95 (accession number NZ_LABM01000017.1) that does carry a functional copy of *plcR-papR*, but the *nprB* gene is absent or truncated (Pomerantsev et al., 2009), suggesting other proteases are capable of fulfilling this role. Temperature-dependent proteolytic activity was observed using the supernatant of *Bc*G9241, suggesting that the processing of PapR by extracellular proteases may be temperature-dependent. From the secretome analysis of *Bc*G9241, AQ16_5,317, a thermolysin metallopeptidase, was found to be one of the most highly expressed proteases at 25°C compared to 37°C. Constitutive expression of AQ16_5,317 led to a slight increase in hemolytic activity at 37°C mid-exponential phase, suggesting that AQ16_5,317 is indeed capable of processing PapR into its mature form leading to the expression of PlcR-regulated toxins. The reason for not observing a similar level of hemolytic activity as observed using the supernatant extracted from 25°C growth culture could be that AQ16_5,317 may require further processing in order to be in its active form or is not stable enough to carry out its function at 37°C. It is also likely that though AQ16_5,317 is able to process PapR and express PlcR-regulated toxins at 37°C, other proteases that have not been studied here may also carry out this function, and therefore further analysis is required. This has been observed in *Bacillus subtilis,* where the proteases subtisillin, Epr, and Vpr have been identified to be involved in the maturation of the Phr signaling peptide (Lanigan-Gerdes et al., 2007). The possibility of other proteases processing immature PapR has been stated by Slamti et al. (2014), though data have not been published to support this statement (Slamti et al., 2014).

Overall, this study reveals that hemolytic and cytolytic activity in *Bc*G9241 is determined by temperature. Lytic activity at 25°C was accompanied by higher levels of PlcR-regulated proteins including Hbl, Nhe, Plc, CytK, and AQ16_5,317, a thermolysin metallopeptidase. Production of these virulence factors at 25°C may be essential for the invasion of invertbrate hosts. As shown in Figure 7, another finding of our work is that the temperature-dependent toxin production is due to differential expression of protease(s) involved in processing the immature PapR into its mature form to be reimported and then activate PlcR. This study suggests that temperature-dependent regulation of the PlcR-PapR regulator allows *Bc*G9241 to accommodate a functional copy of *atxA*. We hypothesize that this has led to the ability of *Bc*G9241 to switch between a *B. cereus*-like phenotype at 25°C and a *B. anthracis*-like phenotype at 37°C. The lower activity of the PlcR regulon at 37°C compared to 25°C could be to allow the expression of AtxA and its regulon, known to be expressed at 37°C in *B. anthracis* (Dai and Koehler, 1997). The characterization of this "cross-over" strain demonstrates that the

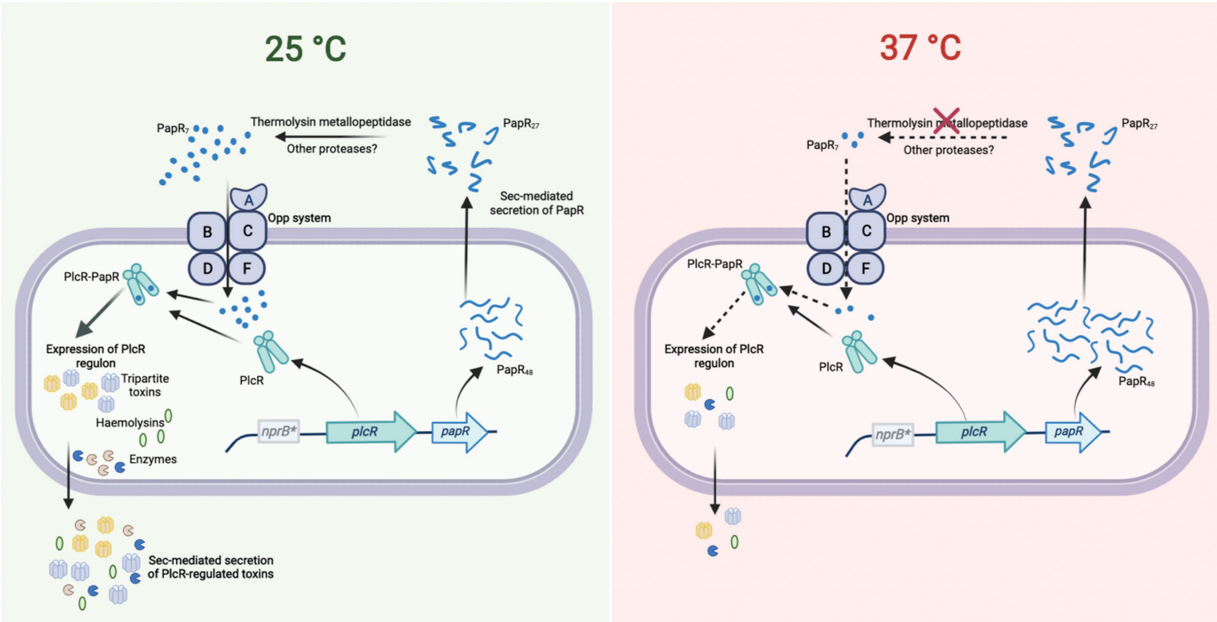

FIGURE 7
The PlcR-PapR regulation circuit in *Bc*G9241 at 25°C and 37°C. In *Bc*G9241, the expression of *plcR* was observed at 25°C and 37°C, suggesting that rather than the expression of the regulator, the activity of the PlcR-PapR active complex is causing differential production of PlcR-regulated toxins. PapR was highly expressed at 37°C compared to 25°C, potentially to compensate for the low expression of the PlcR regulon. Secretion of PapR was observed at both temperatures, suggesting that the Sec machinery is functional at both temperatures. The import system is also functional at both temperatures when $PapR_7$ is available extracellularly. Remnants of the *nprB* gene (*nprB**) are present in *Bc*G9241, thus the protease NprB is not involved in the maturation of PapR as observed in *B. cereus* and *B. thuringiensis*. A PlcR-regulated thermolysin metallopeptidase (AQ16_5,317) was identified to have the ability to process PapR and cause hemolytic activity. AQ16_5,317 is highly expressed at 25°C compared to 37°C. Diagram created with BioRender.com.

evolution of *B. anthracis* as a significant mammalian pathogen is not merely about acquisition of genetic information but is also a story of the power of regulation in controlling potential incompatibilities between incumbent and newly acquired systems which may be a feature of other emerging pathogens.

Materials and methods

Bacterial strains and growth conditions

Bacterial strains used in this study were *Bc*G9241 (Hoffmaster et al., 2004), *Bc*G9241 ΔpBCX01 (Visschedyk et al., 2012), *B. cereus* reference strain ATCC 14579 (American Type Culture Collection, Manassas, Va.), the *plcR*-defective strain *B. thuringiensis* 407 Cry^- Δ*plcR* (Salamitou et al., 2000), and *B. anthracis* Sterne 34F2 ($pXO1^+$, $pXO2^-$). *Bacillus* strains were cultured in 5 mL lysogeny broth (LB) at either 2525C or 37°C overnight before subculturing into 5 mL LB media by diluting the overnight culture to $OD_{600} = 0.005$. All cultures were incubated with shaking at 200 rpm. Larger cultures of *Bacillus* strains were cultured in 50 mL of LB unless otherwise specified. For cloning, *Escherichia coli* DH5-α (NEB) and the methylation deficient *E. coli* ET12567/pUZ8002 (MacNeil et al., 1992) were used in this study. *E. coli* strains were grown in 5 mL LB media at 37°C, shaking at 200 rpm. Media contained antibiotics when appropriate: ampicillin (100 μg/mL), chloramphenicol (25 μg/mL), kanamycin (25 μg/mL) for *E. coli* and erythromycin (25 μg/mL) for *B. cereus* strains.

Hemolysis assay

Hemolytic activity was determined from sheep erythrocytes as described in Rudkin et al. (2014). Briefly, erythrocytes were diluted to 4% (vol/vol), in RPMI-1640 medium and 50 μL of this cell suspension were transferred to a 96-well round-bottom polystyrene plate and incubated with 50 μL of filtered supernatants of *B. cereus* cells grown to exponential ($OD_{600} = 0.5$), early stationary phase ($OD_{600} = 1.5$) or late stationary phase (Supplementary Figure S8; Taylor-Joyce et al., 2023). Following a 1 h-incubation at 37°C, lysis of human/sheep erythrocytes were determined by quantifying the hemoglobin release by measurement of the absorbance at 540 nm in the resulting supernatant. LB and 1% Triton X-100 were used as negative and positive control for 0% lysis and 70% lysis, respectively. %RBC hemolysis was calculated as $(OD_{sample} - OD_{negative\ control})/(OD_{positive\ control} - OD_{negative\ control}) \times 70\%$. Assays were done by triplicate unless otherwise stated.

Protein extraction

Before cultures were seeded for protein extraction, pre-cultures of *Bc*G9241 were used to synchronize bacterial cell growth. Pre-cultures were inoculated into 50 mL of LB broth at $OD_{600} = 0.005$, for protein extraction. Secreted proteins were collected from mid-exponential phase or late stationary phase at both 25°C and 37°C (Taylor-Joyce et al., 2023). Once *Bc*G9241 had grown to the appropriate time point, 6.75 OD units of cells were centrifuged for 5 min at 8000 rpm at 4°C.

Protein extraction for secretome proteomics using in-gel digestion. Supernatant was extracted and acidified to pH 5 using 10% trifluoric acid (TFA). Fifty microliter of StrataClean resin (Agilent) was added to each sample before vortexing for 1 min. All samples were incubated overnight on a rotor wheel mixer overnight at 4°C for efficient protein extraction. StrataClean resin was collected by centrifugation at 870 g for 1 min. Cell supernatant was removed, and the beads resuspended in 100 μL of Laemlli buffer. The suspension was boiled at 95°C for 5 min, to unbind the protein from the resin. Beads were pelleted at 870 g for 1 min and protein-Laemlli buffer suspension collected.

Twenty-five microliter of the secreted proteins were ran on a Mini-PROTEAN® TGX™ precast gel (Bio-Rad). The whole lane of the gel for each sample was sliced into 4 mm sections and washed with 1 mL of 50% ethanol in 50 mM ammonium bicarbonate (ABC). This wash was incubated for 20 min at 55°C, shaking at 650 rpm. The wash solution was removed and this step was repeated twice more. The gel was dehydrated in 400 μL of 100% ethanol by incubation at 55°C for 5 min, with 650 rpm shaking. Once the gel was dehydrated, remaining ethanol was removed. Disulfide bonds were reduced by addition of 300 μL of 10 mM dithiothreitol (DTT) in 50 mM ABC. This was incubated for 45 min at 56°C with 650 rpm shaking. DTT was removed and samples were cooled to room temperature. Cysteine residues were alkylated by adding 300 μL of 55 mM iodoacetamide (IAA) in 50 mM ABC with incubation at room temperature, in the dark for 30 min. IAA was removed and gel was washed as before by adding 1 mL of 50% ethanol in 50 mM and incubated at 55°C for 20 min with shaking at 650 rpm. The ethanol was removed and this wash was repeated twice. Gel pieces were again dehydrated with 400 μL of 100% ethanol and incubated for 5 min at 55°C. Two hundred microliter of trypsin at 2.5 ng μL^{-1} was added to the dehydrated gel and ABC added to ensure the rehydrated gel was fully submerged. The trypsin digest was incubated for 16 h at 37°C with 650 rpm shaking. The digest was stopped by addition of 200 μL 5% formic acid in 25% acetonitrile. The solution was sonicated for 10 min at 35 KHz and the supernatant extracted. This step was repeated three more times. A C18 stage-tip (Thermo Scientific™) was made and conditioned by centrifuging 50 μL 100% methanol through the tip for 2 min at 2000 rpm. 100% acetonitrile was washed through the tip in the same manner to equilibrate it. The tip was further equilibrated with 2% acetonitrile with 1% TFA washed through the tip as before but for 4 min. Samples were then diluted to a concentration of 10 μg of protein in 150 μL final volume of 2% acetonitrile/0.1% TFA. Samples were collected on the stage tip by centrifugation through the stage tip for 10 min under previous spin conditions. The membrane was washed with 50 μL 2% acetonitrile/0.1% TFA by centrifugation at 2000 rpm for 4 min. Peptides were eluted in 20 μL 80% acetonitrile. Samples were dried to a total volume of 40 μL at 40°C in a speed-vac. Samples were resuspended in 55 μL of 2.5% acetonitrile containing 0.05% TFA and sonicated for 30 min at 35 KHz. Samples were dried to a total volume of 40 μL at 40°C in a speed-vac again ready for mass spectroscopy. Nano liquid chromatography-electrospray ionization-mass spectrometry (nanoLC-ESI-MS)/mass spectrometry (MS) was used to carry out the analysis.

Protein extraction for intracellular proteomics using in-urea protein digests. Cell supernatant was removed and cell pellets were suspended in 100 μL of 8 M urea. Suspensions were transferred to Lysing Matrix B tubes (MP Biomedicals) and cells were lysed using the FastPrep®-24 Classic instrument with a COOLPREP™ adapter (MP Biomedicals). Bead beating was conducted at 6 ms^{-1} for 40 s for 2 cycles, with a 300 s pause between cycles. Samples were filtered through nitrocellulose membranes to remove the beads and protein was quantified using a Qubit 2.0 fluorometer and a Qubit™ protein assay kit (Life Technologies). Fifty microgram of protein sample was suspended in 50 μL of 8 M urea buffer. 5.5 μL of 10 mM DTT was added and the samples were incubated for 1 h at room temperature. 6.2 μL of 55 mM IAA was added to samples before 45 min incubation at room temperature in the dark. Samples were then diluted to 100 μL total volume by addition of 50 mM ABC. One microgram of trypsin was added to each sample per 50 μg protein and incubated for 16 h at room temperature. Samples were filtered through a C-18 stage tip as described previously and concentrated to 40 μL in a speed-vac, ready for mass spectroscopy. nanoLC-ESI-MS/MS was used to carry out the analysis.

Perseus analysis of proteomics data

The Perseus software platform (Max Planck Institute) was used to analyze the highly multivariate proteomics data. Peptides only identified by site, reversed peptide sequences and potential contaminants were filtered out. Secretome data was normalized by the mean label-free quantification (LFQ) intensity value. Whole cell proteomics data was normalized by median as the data was normally distributed. Protein hits were filtered out if they did not have 3 values in at least one condition measured. Volcano plots were plotted using a p value = 0.05 and a log2-fold change = 1.

Generation of plasmid-based transcription-translation GFP reporters

Constructs made for this study are listed on Supplementary Table S2. Transcription-translation fusions with the *gfp* gene were constructed by PCR in a pHT315 vector (Lanigan-Gerdes et al., 2007) containing *gfp* (pHT315-*gfp*). The vector was linearized using appropriate restriction enzymes (NEB) and purified after agarose gel electrophoresis using the GFX™ PCR DNA and Gel Band Purification Kit (GE Healthcare). Insert fragments were amplified with Q5 DNA polymerase (NEB) by PCR with the appropriate primer pairs listed on Supplementary Table S3. The resulting fragments were digested with the appropriate restriction enzymes, purified after agarose gel electrophoresis using the GFX™ PCR DNA and Gel Band Purification Kit (GE Healthcare) and ligated into the linearized pHT315-*gfp* vector. Plasmid constructs were transformed into chemically competent *E. coli* DH5-α cells through heat shock. Once confirmed by DNA sequencing, all vectors were transformed into the non-methylating *E. coli* ET12567 strain by electroporation (Supplementary Materials and Methods). Vectors amplified by *E. coli* ET12567 were purified and transformed into *B. cereus* strains using electroporation (Supplementary Materials and Methods).

Fluorescent reporter strain assays

For growth curves and fluorescence measurements, *B. cereus* strains were sub-cultured at a starting OD_{600} of 0.05 into a clear flat bottom 96-well plate (Greiner) containing 100 μL of LB media per well. Cultures were grown in a FLUOstar Omega microplate reader (BMG LabTech) at either 25°C or 37°C with continuous orbital shaking at 700 rpm. Absorbance measurements (OD_{600}) and fluorescence intensity (excitation filter = 482 nm and emission

filter = 520 nm for GFP) were taken hourly for 24 h. Each plate contained *Bc*G9241 and *Bc*ATCC14579 strains carrying GFP reporters as well as each strain carrying a control plasmid with no promoter upstream of *gfp* (pHT315-*gfp*). The fluorescence of all readings was first normalized to the fluorescence of blank media samples and then normalized by subtracting the autofluorescence of the corresponding control strain. The rate of change in fluorescence ($\Delta GFP/OD_{600}$) using the data obtained from the microplate reader was calculated by subtracting the fluorescence at a given time point by the fluorescence of the previous time point:

$$\Delta GFP / OD_{600} = \left(GFP\ intensity_{(t)} - GFP\ intensity_{(t-1)}\right) / OD_{600}.$$

Peptide synthesis

Peptides SDLPFEH (G9241 $PapR_7$) and KDLPFEY (ATCC14579 $PapR_7$) were synthesized by GenScript (United States) at a purity >98% and diluted with sterile nuclease-free water. All experiments with the use of $PapR_7$ were added at a concentration of 10 μM and during lag growth phase ($OD_{600} = 0.1$), unless otherwise stated.

Light and fluorescence microscopy

One percent agarose in water were made and heated using a microwave until the agarose has completely dissolved. 200 μL of molten agarose was added onto a microscope glass slide and a coverslip placed on top. When the agarose pad has dried and the sample is ready for observation, 2 μL of sample was applied to a prepared agarose pad and a cover slip placed over them. Images were captured on a Leica DMi8 premium-class modular research microscope with a Leica EL6000 external light source (Leica Microsystems), using an ORCA-Flash4.0 V2 Digital CMOS Camera (Hamamatsu) at 100x magnification.

$PapR_7$ activity assay using PlcR-regulated toxin reporters

*Bc*G9241 and *Bc*ATCC14579 containing PlcR-regulated toxin GFP reporters were grown overnight in LB medium with selective antibiotics. Mid-exponentially grown pre-cultures of *B. cereus* strains containing PlcR-regulated toxin reporters were diluted to OD_{600} 0.01 and 10 μM of $PapR_7$ were added. In a black tissue culture treated 96-well microtiter plate (Greiner, Scientific Laboratory Supplies), 100 μL of the culture were added in each well and the GFP intensity and OD_{600} were measured every hour for over 24 h using the Omega FluoSTAR (BMG LabTech) microplate reader.

Data availability statement

The original contributions presented in the study are included in the article/Supplementary material, further inquiries can be directed to the corresponding author.

Author contributions

SM planned and performed experiments and wrote much of the manuscript. GT-J assisted in experiments and wrote parts of the manuscript. TB and CH-R planned and performed some of the experiments. LB provided certain bacterial strains and provided advice on handling them. PO and VB provided advice on handling the pathogenic strains and assisted in interpreting the results. AH assisted in some experimental work and in interpreting certain results. NW experimental planning, secured funding, assisted in interpreting results, and provided guidance and edits for writing the manuscript. All authors contributed to the article and approved the submitted version.

Funding

SM and TB were funded by the WCPRS scholarship programme provided by Warwick University, with funding contributions from Dstl (MoD) at Porton Down, UK (DSTL project references; DSTLX1000093952 and DSTLX-1000128995). GT-J was funded by the BBSRC MIBTP Doctoral Training Programme at the University of Warwick, UK. CH-R was funded by an EU Marie Curie fellowship awarded while at the University of Bath, UK (FP7-PEOPLE-2010-IEF Project 273155). AH was funded by a start-up financial package awarded to NW upon starting at Warwick Medical School, UK. LB is funded by Cardiff School of Biological Sciences, UK. PO is funded by Dstl at Porton Down, UK. NW is funded by the University of Warwick, UK.

Acknowledgments

We would like to thank the Dstl for providing funding and guidance throughout the project including valuable quarterly update meetings. We would also like to acknowledge the contribution of the WPH Proteomics Research Technology Platform (Gibbet Hill Road, University of Warwick, UK).

Conflict of interest

The authors declare that the research was conducted in the absence of any commercial or financial relationships that could be construed as a potential conflict of interest.

Publisher's note

All claims expressed in this article are solely those of the authors and do not necessarily represent those of their affiliated organizations, or those of the publisher, the editors and the reviewers. Any product that may be evaluated in this article, or claim that may be made by its manufacturer, is not guaranteed or endorsed by the publisher.

Supplementary material

The Supplementary material for this article can be found online at: https://www.frontiersin.org/articles/10.3389/fmicb.2023.1113562/full#supplementary-material

References

Agaisse, H., Gomlnet, M., Økstad, O. A., Kolstø, A. B., and Lereclus, D. (1999). PlcR is a pleiotropic regulator of extracellular virulence factor gene expression in *Bacillus thuringiensis*. *Mol. Microbiol.* 32, 1043–1053. doi: 10.1046/j.1365-2958.1999.01419.x

Antonation, K. S., Grützmacher, K., Dupke, S., Mabon, P., Zimmermann, F., Lankester, F., et al. (2016). *Bacillus cereus* Biovar *anthracis* causing anthrax in sub-Saharan Africa—chromosomal Monophyly and broad geographic distribution. *PLoS Negl. Trop. Dis.* 10, 1–14. doi: 10.1371/journal.pntd.0004923

Avashia, S. B., Riggins, W. S., Lindley, C., Hoffmaster, A., Drumgoole, R., Nekomoto, T., et al. (2007). Fatal pneumonia among metalworkers due to inhalation exposure to *Bacillus cereus* containing *Bacillus anthracis* toxin genes. *Clin. Infect. Dis.* 44, 414–416. doi: 10.1086/510429

Baldwin, V. M. (2020). You Can't B cereus – a review of *Bacillus cereus* strains that cause anthrax-like disease. *Front. Microbiol.* 11:1731. doi: 10.3389/fmicb.2020.01731

Bouillaut, L., Perchat, S., Arold, S., Zorrilla, S., Slamti, L., Henry, C., et al. (2008). Molecular basis for group-specific activation of the virulence regulator PlcR by PapR heptapeptides. *Nucleic Acids Res.* 36, 3791–3801. doi: 10.1093/nar/gkn149

Brillard, J., Susanna, K., Michaud, C., Dargaignaratz, C., Gohar, M., Nielsen-Leroux, C., et al. (2008). The YvfTU two-component system is involved in plcR expression in *Bacillus cereus*. *BMC Microbiol.* 8, 183–113. doi: 10.1186/1471-2180-8-183

Carter, K. C. (1985). Koch's postulates in relation to the work of Jacob Henle and Edwin Klebs. *Med. Hist.* 29, 353–374. doi: 10.1017/S0025727300044689

Ceuppens, S., Timmery, S., Mahillon, J., Uyttendaele, M., and Boon, N. (2012). Small *Bacillus cereus* ATCC 14579 subpopulations are responsible for cytotoxin K production. *J. Appl. Microbiol.* 114, 899–906. doi: 10.1111/jam.12096

Dai, Z., and Koehler, T. M. (1997). Regulation of anthrax toxin activator gene (atxA) expression in *Bacillus anthracis*: temperature, not CO2/bicarbonate affects AtxA synthesis. *Infect Immun.* 65, 2576–2582. doi: 10.1128/iai.65.7.2576-2582.1997

Dawson, P., Schrodt, C. A., Feldmann, K., Traxler, R. M., Gee, J. E., Kolton, C. B., et al. (2021). Fatal anthrax pneumonia in welders and other metalworkers caused by *Bacillus cereus* group bacteria containing anthrax toxin genes — U.S. Gulf Coast states, 1994–2020. *Morb. Mortal. Wkly Rep.* 70, 1453–1454. doi: 10.15585/mmwr.mm7041a4

Declerck, N., Bouillaut, L., Chaix, D., Rugani, N., Slamti, L., Hoh, F., et al. (2007). Structure of PlcR: insights into virulence regulation and evolution of quorum sensing in gram-positive bacteria. *PNAS* 104, 18490–18495. doi: 10.1073/pnas.0704501104

Dupke, S., Barduhn, A., Franz, T., Leendertz, F. H., Couacy-Hymann, E., Grunow, R., et al. (2019). Analysis of a newly discovered antigen of *Bacillus cereus* biovar *anthracis* for its suitability in specific serological antibody testing. *J. Appl. Microbiol.* 126, 311–323. doi: 10.1111/jam.14114

Duport, C., Zigha, A., Rosenfeld, E., and Schmitt, P. (2006). Control of enterotoxin gene expression in *Bacillus cereus* F4430/73 involves the redox-sensitive ResDE signal transduction system. *J. Bacteriol.* 188, 6640–6651. doi: 10.1128/JB.00702-06

Esbelin, J., Jouanneau, Y., and Duport, C. (2012). *Bacillus cereus* Fnr binds a [4Fe-4S] cluster and forms a ternary complex with ResD and PlcR. *BMC Microbiol.* 12, 1–9. doi: 10.1186/1471-2180-12-125

Fagerlund, A., Lindbäck, T., Storset, A. K., Granum, P. E., and Hardy, S. P. (2008). *Bacillus cereus* Nhe is a pore-forming toxin with structural and functional properties similar to the ClyA (HlyE, SheA) family of haemolysins, able to induce osmotic lysis in epithelia. *Microbiology* 154, 693–704. doi: 10.1099/mic.0.2007/014134-0

Fieldhouse, R. J., Turgeon, Z., White, D., and Rod, M. A. (2010). Cholera-and anthrax-like toxins are among several new ADP-Ribosyltransferases. *PLoS Comput. Biol.* 6:e1001029. doi: 10.1371/journal.pcbi.1001029

Gilmore, M. S., Cruz-Rodz, A. L., Leimeister-Wachter, M., Kreft, J., and Goebel, W. (1989). A *Bacillus cereus* cytolytic determinant, cereolysin AB, which comprises the phospholipase C and sphingomyelinase genes: nucleotide sequence and genetic linkage. *J. Bacteriol.* 171, 744–753. doi: 10.1128/jb.171.2.744-753.1989

Gohar, M., Faegri, K., Perchat, S., Ravnum, S., Økstad, O. A., Gominet, M., et al. (2008). The PlcR virulence regulon of *Bacillus cereus*. *PLoS One* 3, 1–9. doi: 10.1371/journal.pone.0002793

Gohar, M., Økstad, O. A., Gilois, N., Sanchis, V., Kolstø, A. B., and Lereclus, D. (2002). Two-dimensional electrophoresis analysis of the extracellular proteome of *Bacillus cereus* reveals the importance of the PlcR regulon. *Proteomics* 2, 784–791.

Gominet, M., Slamti, L., Gilois, N., Rose, M., Lereclus, D., and Universita, È. (2001). Oligopeptide permease is required for expression of the *Bacillus thuringiensis* PlcR regulon and for virulence. *Mol. Microbiol.* 40, 963–975. doi: 10.1046/j.1365-2958.2001.02440.x

Granum, P. E., and Lund, T. (1997). *Bacillus cereus* and its food poisoning toxins. *FEMS Microbiol. Lett.* 157, 223–228. doi: 10.1111/j.1574-6968.1997.tb12776.x

Grenha, R., Slamti, L., Nicaise, M., Refes, Y., Lereclus, D., and Nessler, S. (2013). Structural basis for the activation mechanism of the PlcR virulence regulator by the quorum-sensing signal peptide PapR. *PNAS* 110, 1047–1052. doi: 10.1073/pnas.1213770110

Hendrix, R. W., Casjens, S. R., and Lavigne, R. (2012). Family - Siphoviridae. *Virus Taxon.* 2012, 86–98. doi: 10.1016/B978-0-12-384684-6.00004-5

Hoffmaster, A. R., Hill, K. K., Gee, J. E., Marston, C. K., De, B. K., Popovic, T., et al. (2006). Characterization of *Bacillus cereus* isolates associated with fatal pneumonias: strains are closely related to *Bacillus anthracis* and harbor *B. anthracis* virulence genes. *J. Clin. Microbiol.* 44, 3352–3360. doi: 10.1128/JCM.00561-06

Hoffmaster, A. R., Ravel, J., Rasko, D. A., Chapman, G. D., Chute, M. D., Marston, C. K., et al. (2004). Identification of anthrax toxin genes in a *Bacillus cereus* associated with an illness resembling inhalation anthrax. *PNAS* 101, 8449–8454. doi: 10.1073/pnas.0402414101

Klee, S. R., Brzuszkiewicz, E. B., Nattermann, H., Brüggemann, H., Dupke, S., Wollherr, A., et al. (2010). The genome of a *Bacillus* isolate causing anthrax in chimpanzees combines chromosomal properties of B. cereus with B. anthracis virulence plasmids. *PLoS One* 5:e10986. doi: 10.1371/journal.pone.0010986

Lanigan-Gerdes, S., Dooley, A. N., Faull, K. F., and Lazazzera, B. A. (2007). Identification of subtilisin, Epr and Vpr as enzymes that produce CSF, an extracellular signalling peptide of Bacillus subtilis. *Mol. Microbiol.* 65, 1321–1333. doi: 10.1111/j.1365-2958.2007.05869.x

Leendertz, F. H., Ellerbrok, H., Boesch, C., Couacy-Hymann, E., Mätz-Rensing, K., Hakenbeck, R., et al. (2004). Anthrax kills wild chimpanzees in a tropical rainforest. *Nature* 430, 451–452. doi: 10.1038/nature02722

Leendertz, F. H., Lankester, F., Guislain, P., Neel, C., and Drori, O. (2006a). Anthrax in Western and central African great apes. *Am. J. Primatol.* 68, 928–933. doi: 10.1002/ajp.20298

Leendertz, F. H., Yumlu, S., Pauli, G., Boesch, C., Couacy-Hymann, E., Vigilant, L., et al. (2006b). A new *Bacillus anthracis* found in wild chimpanzees and a gorilla from west and Central Africa. *PLoS Pathog.* 2, 0001–0004. doi: 10.1371/journal.ppat.0020008

Lereclus, D., Agaisse, H., Gominet, M., Salamitou, S., and Sanchis, V. (1996). Identification of a *Bacillus thuringiensis* gene that positively regulates transcription of the phosphatidylinositol-specific phospholipase C gene at the onset of the stationary phase. *J. Bacteriol.* 178, 2749–2756. doi: 10.1128/jb.178.10.2749-2756.1996

Lereclus, D., Agaisse, H., Salamitou, S., and Gominet, M. (2000). Regulation of toxin and virulence gene transcription in *Bacillus thuringiensis*. *Int. J. Med. Microbiol.* 290, 295–299. doi: 10.1016/S1438-4221(00)80024-7

Lund, T., De Buyser, M.-L., and Granum, P. E. (2000). A new cytotoxin from *Bacillus cereus* that may cause necrotic enteritis. *Mol. Microbiol.* 38, 254–261. doi: 10.1046/j.1365-2958.2000.02147.x

Lund, T., and Granum, P. E. (1996). Characterisation of a non-haemolytic enterotoxin complex from *Bacillus cereus* isolated after a foodborne outbreak. *FEMS Microbiol. Lett.* 141, 151–156. doi: 10.1111/j.1574-6968.1996.tb08377.x

MacNeil, D. J., Gewain, K. M., Ruby, C. L., Dezeny, G., Gibbons, P. H., and MacNeil, T. (1992). Analysis of Streptomyces avermitilis genes required for avermectin biosynthesis utilizing a novel integration vector. *Gene* 111, 61–68. doi: 10.1016/0378-1119(92)90603-M

Marston, C. K., Ibrahim, H., Lee, P., Churchwell, G., Gumke, M., Stanek, D., et al. (2016). Anthrax toxin-expressing *Bacillus cereus* isolated from an anthrax-like eschar. *PLoS One* 11, 1–7. doi: 10.1371/journal.pone.0156987

Mignot, T., Mock, M., Robichon, D., Landier, A., Lereclus, D., and Fouet, A. (2001). The incompatibility between the PlcR-and AtxA-controlled regulons may have selected a nonsense mutation in *Bacillus anthracis*. *Mol. Microbiol.* 42, 1189–1198. doi: 10.1046/j.1365-2958.2001.02692.x

Miller, J. M., Hair, J. G., Hebert, M., Hebert, L., Roberts, F. J. Jr., and Weyant, R. S. (1997). Fulminating bacteremia and pneumonia due to *Bacillus cereus*. *J. Clin. Microbiol.* 35, 504–507. doi: 10.1128/jcm.35.2.504-507.1997

Okinaka, R., and Keim, P. (2016). The phylogeny of *Bacillus cereus* sensu lato. *Microbiol. Spectr.* 4:TBS-0012-2012. doi: 10.1128/microbiolspec.TBS-0012-2012

Økstad, O. A., Gominet, M., Purnelle, B., Rose, M., Lereclus, D., and Kolsto, A.-B. (1999). Sequence analysis of three *Bacillus cereus* loci carrying PlcR-regulated genes encoding degradative enzymes and enterotoxin. *Microbiology* 145, 3129–3138. doi: 10.1099/00221287-145-11-3129

Passalacqua, K. D., Varadarajan, A., Byrd, B., and Bergman, N. H. (2009). Comparative transcriptional profiling of *Bacillus cereus sensu lato* strains during growth in CO2-bicarbonate and aerobic atmospheres. *PLoS One* 4, 1–20. doi: 10.1371/journal.pone.0004904

Pena-Gonzalez, A., Marston, C. K., Rodriguez-R, L. M., Kolton, C. B., Garcia-Diaz, J., Theppote, A., et al. (2017). Draft genome sequence of *Bacillus cereus* LA2007, a human-pathogenic isolate harboring anthrax-like plasmids. *Genome Announc. [Internet].* 5:e00181-17. doi: 10.1128/genomeA.00181-17

Pomerantsev, A. P., Kalnin, K. V., Osorio, M., and Leppla, S. H. (2003). Phosphatidylcholine-specific phospholipase C and sphingomyelinase activities in bacteria of the *Bacillus cereus* group. *Infect. Immun.* 71, 6591–6606. doi: 10.1128/IAI.71.11.6591-6606.2003

Pomerantsev, A. P., Pomerantseva, O. M., Camp, A. S., Mukkamala, R., Goldman, S., and Leppla, S. H. (2009). PapR peptide maturation: role ofthe NprB protease in *Bacillus cereus* 569 PlcR / PapR global gene regulation. *FEMS Immunol. Med. Microbiol.* 55, 361–377. doi: 10.1111/j.1574-695X.2008.00521.x

Pomerantsev, A. P., Pomerantseva, O. M., and Leppla, S. H. (2004). A spontaneous translational fusion of *Bacillus cereus* PlcR and PapR activates transcription of PlcR-

dependent genes in *Bacillus anthracis* via binding with a specific palindromic sequence. *Infect. Immun.* 72, 5814–5823. doi: 10.1128/IAI.72.10.5814-5823.2004

Réjasse, A., Gilois, N., Barbosa, I., Huillet, E., Bevilacqua, C., Tran, S., et al. (2012). Temperature-dependent production of various PlcR-controlled virulence factors in *Bacillus weihenstephanensis* strain KBAB4. *Appl. Environ. Microbiol.* 78, 2553–2561. doi: 10.1128/AEM.07446-11

Rivera, A. M. G., Granum, P. E., and Priest, F. G. (2000). Common occurrence of enterotoxin genes and enterotoxicity in *Bacillus thuringiensis*. *FEMS Microbiol. Lett.* 190, 151–155. doi: 10.1111/j.1574-6968.2000.tb09278.x

Rudkin, J. K., Laabei, M., Edwards, A. M., Joo, H. S., Otto, M., Lennon, K. L., et al. (2014). Oxacillin alters the toxin expression profile of community-associated methicillin-resistant *Staphylococcus aureus*. *Antimicrob. Agents Chemother.* 58, 1100–1107. doi: 10.1128/AAC.01618-13

Salamitou, S., Brehe, M., Bourguet, D., Gilois, N., Gominet, M., and Hernandez, E. (2000). The plcR regulon is involved in the opportunistic properties of *Bacillus thuringiensis* and *Bacillus cereus* in mice and insects. *Microbiology* 146, 2825–2832. doi: 10.1099/00221287-146-11-2825

Slamti, L., Gominet, M., Vilas-bo, G., Sanchis, V., Chaufaux, J., Gohar, M., et al. (2004). Distinct mutations in PlcR explain why some strains of the *Bacillus cereus* group are nonhemolytic. *J. Bacteriol.* 186, 3531–3538. doi: 10.1128/JB.186.11.3531-3538.2004

Slamti, L., Lemy, C., Henry, C., Guillot, A., Huillet, E., and Lereclus, D. (2016). CodY regulates the activity of the virulence quorum sensor PlcR by controlling the import of the signaling peptide PapR in *Bacillus thuringiensis*. *Front. Microbiol.* 6, 1–14. doi: 10.3389/fmicb.2015.01501

Slamti, L., and Lereclus, D. (2002). A cell-cell signaling peptide activates the PlcR virulence regulon in bacteria of the *Bacillus cereus* group. *EMBO J.* 21, 4550–4559. doi: 10.1093/emboj/cdf450

Slamti, L., and Lereclus, D. (2005). Specificity and polymorphism of the PlcR-PapR quorum-sensing system in the *Bacillus cereus* group. *J. Bacteriol.* 187, 1182–1187. doi: 10.1128/JB.187.3.1182-1187.2005

Slamti, L., Perchat, S., Huillet, E., and Lereclus, D. (2014). Quorum sensing in *Bacillus thuringiensis* is required for completion of a full infectious cycle in the insect. *Toxins (Basel).* 6, 2239–2255. doi: 10.3390/toxins6082239

Sue, D., Hoffmaster, A. R., Popovic, T., and Wilkins, P. P. (2006). Capsule production in *Bacillus cereus* strains associated with severe pneumonia. *J. Clin. Microbiol.* 44, 3426–3428. doi: 10.1128/JCM.00873-06

Swiecicka, I., and Mahillon, J. (2006). Diversity of commensal *Bacillus cereus* sensu lato isolated from the common sow bug (Porcellio scaber, isopoda). *FEMS Microbiol. Ecol.* 56, 132–140. doi: 10.1111/j.1574-6941.2006.00063.x

Swiecicka, I., Van Der Auwera, G. A., and Mahillon, J. (2006). Hemolytic and nonhemolytic enterotoxin genes are broadly distributed among *Bacillus thuringiensis* isolated from wild mammals. *Microb. Ecol.* 52, 544–551. doi: 10.1007/s00248-006-9122-0

Taylor-Joyce, G., Manoharan, S., Brooker, T., Hernandez-Rodrıguez, C. S., Baillie, L., Oyston, P., et al. (2023). The influence of extrachromosomal elements in the anthrax "cross-over" strain *Bacillus cereus* G9241. *Front. Microbio*. 14:1113642. doi: 10.3389/fmicb.2023.1113642

Vilain, S., Luo, Y., Hildreth, M. B., and Brözel, V. S. (2006). Analysis of the life cycle of the soil saprophyte *Bacillus cereus* in liquid soil extract and in soil. *Appl. Environ. Microbiol.* 72, 4970–4977. doi: 10.1128/AEM.03076-05

Visschedyk, D., Rochon, A., Tempel, W., Dimov, S., Park, H. W., and Merrill, A. R. (2012). Certhrax toxin, an anthrax-related ADP-ribosyltransferase from *Bacillus cereus*. *J. Biol. Chem.* 287, 41089–41102. doi: 10.1074/jbc.M112.412809

Wright, A. M., Beres, S. B., Consamus, E. N., Long, S. W., Flores, A. R., Barrios, R., et al. (2011). Rapidly progressive, fatal, inhalation anthrax-like infection in a human: case report, pathogen genome sequencing, pathology, and coordinated response. *Arch. Pathol. Lab. Med.* 135, 1447–1459. doi: 10.5858/2011-0362-SAIR.1

Zigha, A., Rosenfeld, E., Schmitt, P., and Duport, C. (2007). The redox regulator Fnr is required for fermentative growth and enterotoxin synthesis in *Bacillus cereus* F4430/73. *J. Bacteriol.* 189, 2813–2824. doi: 10.1128/JB.01701-06